

Manuscript Number:

Title: A multi-instrumental geochemical approach to assess the environmental impact of CO<sub>2</sub>-rich gas emissions in a densely populated area: the case of Cava dei Selci (Latium, Italy)

Article Type: Research Paper

Keywords: CO<sub>2</sub> diffuse degassing; air quality; Cava dei Selci; Colli Albani; gas hazard.

Corresponding Author: Dr. Stefania Venturi,

Corresponding Author's Institution: National Research Council of Italy (CNR)

First Author: Stefania Venturi

Order of Authors: Stefania Venturi; Franco Tassi; Jacopo Cabassi; Orlando Vaselli; Ilaria Minardi; Simone Neri; Chiara Caponi; Giorgio Capasso; Roberto Di Martino; Andrea Ricci; Francesco Capecchiacci; Matteo Lelli; Alessandra Sciarra; Daniele Cinti; Giorgio Virgili

Abstract: The Colli Albani volcanic complex (Lazio, Italy) shows areas (e.g. Tivoli, Cava dei Selci, Tor Caldara, Solforata) characterized by anomalously high emissions of CO<sub>2</sub>-rich gases from soils. The source of these gases is a regional aquifer hosted within the Mesozoic carbonate rock sequences. These gas manifestations, characterized by significant concentrations of H<sub>2</sub>S and other toxic gases (e.g. GEM: Gaseous Elemental Mercury, and Rn), represent a serious hazard for local inhabitants, especially where residential areas such as Cava dei Selci, near Rome (Italy), are located close to emitting areas. In April 2016, a geochemical survey was carried out in an abandoned stone quarry nearby the urban settlement aimed to: (i) investigate the composition of gases emitted from punctual discharges and the anomalously high diffuse soil degassing that characterized the study site, and (ii) evaluate the environmental impact that such gas discharges have on the local air quality. The spatial distribution of the soil CO<sub>2</sub> fluxes was mainly dependent on the local geostructural setting, whereas shallow secondary processes (e.g. oxidation and gas-water interaction) seem to represent the main controlling factor of reactive and/or water-soluble gas species, such as CH<sub>4</sub> and H<sub>2</sub>S. The total output of CO<sub>2</sub> from the abandoned stone quarry accounted for 0.53 % of total CO<sub>2</sub> discharged from the whole Colli Albani volcanic district. The naturally emitted toxic gases (e.g. CO<sub>2</sub>, H<sub>2</sub>S, CH<sub>4</sub>, GEM) largely affect the air quality and, as recorded in the past, are a threat for the human health in both the quarry and the nearby residential area. A mobile multi-instrumental station able to continuously and simultaneously acquire CO<sub>2</sub>, H<sub>2</sub>S, SO<sub>2</sub>, CH<sub>4</sub>, GEM and CO was deployed to verify the concentrations of both the main deep-originated gas compounds and potential secondary gaseous contaminants (i.e. SO<sub>2</sub>) throughout the urban settlement most exposed to the lethal gases. Hydrogen sulfide was found to be the most impacting gas, occasionally exceeding the 24-h air quality guideline for ambient air and

causing odor annoyance among inhabitants at a distance up to more than 250 m downwind from the emitting area. Toxic gas accumulation up to hazardous levels was recognized in poorly ventilated basements, producing anomalous outdoor air concentrations at the street level in front of the descending vehicular access to private garages even relatively far from the main emitting area. The geochemical survey carried out via the mobile multi-instrumental station and soil gas measurements resulted to be particularly efficient for evaluating the potential effects caused by gas emissions in inhabited areas and a pivotal tool for managing future urban development plans.

Suggested Reviewers: Sergio Calabrese  
sergio.calabrese@gmail.com

Cynthia Werner  
cwerner@usgs.gov

Luca Tarchini  
luca.tarchini@uniroma3.it

Francesco Frondini  
francesco.frondini@unipg.it

Georges Vougioukalakis  
gvoug@igme.gr



Stefania Venturi  
Institute of Geosciences and Earth Resources (IGG),  
National Research Council of Italy (CNR)  
Via La Pira 4, 50121, Florence, Italy

Dear Editor,

We are pleased to submit to *Applied Geochemistry* the research paper titled: “*A multi-instrumental geochemical approach to assess the environmental impact of CO<sub>2</sub>-rich gas emissions in a densely populated area: the case of Cava dei Selci (Latium, Italy)*” by Stefania VENTURI, Franco TASSI, Jacopo CABASSI, Orlando VASELLI, Ilaria MINARDI, Simone NERI, Chiara CAPONI, Giorgio CAPASSO, Roberto M.R. Di Martino, Andrea RICCI, Francesco CAPECCHIACCI, Matteo LELLI, Alessandra SCIARRA, Daniele CINTI and Giorgio VIRGILI.

In this paper, we present the results of a geochemical survey carried out at Cava dei Selci (Colli Albani volcanic complex, central Italy). The study area is characterized by the presence of anomalously high emissions of CO<sub>2</sub>-rich gases, through both punctual gas vents and diffuse degassing soils, which occur in close proximity to a densely inhabited residential area. Besides CO<sub>2</sub>, other toxic gases (e.g. H<sub>2</sub>S, CH<sub>4</sub> and GEM) are present at significant concentrations in local gas manifestations. The close proximity of the emitting area to the houses of Cava dei Selci poses a serious threat to local inhabitants. Indeed, several lethal accidents, which were caused by gas inhalation, occurred in the past. Cava dei Selci is not an isolated case, since the Colli Albani volcanic complex is characterized by the copresence of some of the most densely populated municipalities of central Italy and a number of natural gas manifestations. The resulting severe environmental concerns related to both short- and long-term exposure to toxic endogenous gases require the adoption of a proper methodological approach for a correct assessment of the hazard to human health and the definition of intervention plans.

We propose a methodological approach based on a multi-parametric geochemical survey for (i) the characterization of gas emissions from diffuse degassing areas and (ii) the estimation of their impact on local air quality. The chemical analysis of endogenous gases both (i) emitted from punctual discharges and (ii) permeating the soil at shallow depths in areas of anomalous degassing revealed compositional differences related to chemical rearrangements induced by gas-water interaction processes, microbial activity and increasingly oxidizing conditions at shallow depths. Therefore, the processes occurring during fluids motion through the soil are able to control the effective amounts of endogenous gas species discharged into the atmosphere through diffuse degassing.



Measurements of soil CO<sub>2</sub>, H<sub>2</sub>S and CH<sub>4</sub> fluxes were performed, allowing the evaluation of the total outputs of these gases from the diffuse degassing area.

The air quality was estimated both (i) at fixed measuring stations positioned within the emitting areas and (ii) within the near urban settlement. A mobile multi-instrumental station (MMS) able to acquire real-time continuous measurements of air concentrations of CO<sub>2</sub>, H<sub>2</sub>S, SO<sub>2</sub>, CH<sub>4</sub>, GEM and CO was deployed to verify the concentrations of both the main deep-originated gas compounds and potential secondary gaseous contaminants (i.e. SO<sub>2</sub>) throughout the residential area most exposed to the lethal gases. Hydrogen sulfide was found to be the most impacting gas, whilst CO<sub>2</sub>, H<sub>2</sub>S and CH<sub>4</sub> accumulation up to potentially hazardous levels was recognized in poorly ventilated basements.

The proposed methodological approach, based on geochemical survey including soil gas measurements and MMS deployment, is particularly efficient for evaluating the potential effects caused by natural gas emissions in densely inhabited areas and a pivotal tool for managing automated gas sensor monitoring networks and future urban development plans.

This study does not involve human or animal subjects.

All of the authors have read and approved the paper and it has not been published previously nor it is being considered by any other peer-reviewed journal.

Please address all correspondence concerning this manuscript to: [stefania.venturi@igg.cnr.it](mailto:stefania.venturi@igg.cnr.it).

Best regards.

On the behalf of all the Authors,  
Stefania Venturi

## Highlights

- Natural gas emissions and air quality at Cava dei Selci were investigated.
- Processes in the soil affected diffuse emissions of endogenous gases.
- A mobile multi-instrumental station (MMS) was deployed for air quality measurement.
- H<sub>2</sub>S was the most impacting gas in the residential area.
- The MMS is a pivotal tool for managing future monitoring and intervention plans.

1  
2  
3  
4  
5  
6  
7  
8  
9  
10  
11  
12  
13  
14  
15  
16  
17  
18  
19  
20  
21  
22  
23  
24  
25  
26  
27  
28  
29  
30  
31  
32  
33  
34  
35  
36  
37  
38  
39  
40  
41  
42  
43  
44  
45  
46  
47  
48  
49  
50  
51  
52  
53  
54  
55  
56  
57  
58  
59  
60  
61  
62  
63  
64  
65

# A multi-instrumental geochemical approach to assess the environmental impact of CO<sub>2</sub>-rich gas emissions in a densely populated area: the case of Cava dei Selci (Latium, Italy)

S. Venturi<sup>a\*</sup>, F. Tassi<sup>a,b</sup>, J. Cabassi<sup>a</sup>, O. Vaselli<sup>a,b</sup>, I. Minardi<sup>c</sup>, S. Neri<sup>c</sup>, C. Caponi<sup>b</sup>, G. Capasso<sup>d</sup>,  
R.M.R. Di Martino<sup>d</sup>, A. Ricci<sup>e</sup>, F. Capecchiacci<sup>b</sup>, M. Lelli<sup>f</sup>, A. Sciarra<sup>g</sup>, D. Cinti<sup>g</sup>, G. Virgili<sup>c</sup>

<sup>a</sup>*Institute of Geosciences and Earth Resources (IGG), National Research Council of Italy (CNR), Via G. La Pira 4, 50121 Florence (Italy)*

<sup>b</sup>*Department of Earth Sciences, University of Florence, Via G. La Pira 4, 50121 Florence (Italy)*

<sup>c</sup>*West Systems Co. Ltd., Via Don Mazzolari 25, 56025 Pontedera (Italy)*

<sup>d</sup>*Istituto Nazionale di Geofisica e Vulcanologia, Sezione di Palermo, Via Ugo La Malfa 153, 90146 Palermo (Italy)*

<sup>e</sup>*Department of Biological, Geological and Environmental Sciences, University of Bologna, Porta S. Donato 1, 40136 Bologna (Italy)*

<sup>f</sup>*Institute of Geosciences and Earth Resources (IGG), National Research Council of Italy (CNR), Via G. Moruzzi 1, 56124 Pisa (Italy)*

<sup>g</sup>*National Institute of Geophysics and Volcanology (INGV), Via di Vigna Murata 605, 00143 Rome (Italy)*

\* Corresponding author. Institute of Geosciences and Earth Resources (IGG), National Research Council of Italy (CNR), Via G. La Pira 4, 50121, Florence (Italy). Tel: +39 055 2757507; fax: +39 055 284571. E-mail: stefania.venturi@igg.cnr.it.

Submitted to *Applied Geochemistry*

## Abstract

The Colli Albani volcanic complex (Lazio, Italy) shows areas (e.g. Tivoli, Cava dei Selci, Tor Caldara, Solforata) characterized by anomalously high emissions of CO<sub>2</sub>-rich gases from soils. The source of these gases is a regional aquifer hosted within the Mesozoic carbonate rock sequences. These gas manifestations, characterized by significant concentrations of H<sub>2</sub>S and other toxic gases (e.g. GEM: Gaseous Elemental Mercury, and Rn), represent a serious hazard for local inhabitants, especially where residential areas such as Cava dei Selci, near Rome (Italy), are located close to emitting areas. In April 2016, a geochemical survey was carried out in an abandoned stone quarry nearby the urban settlement aimed to: (i) investigate the composition of gases emitted from punctual discharges and the anomalously high diffuse soil degassing that characterized the study site, and (ii) evaluate the environmental impact that such gas discharges have on the local air quality. The spatial distribution of the soil CO<sub>2</sub> fluxes was mainly dependent on the local geostructural setting, whereas shallow secondary processes (e.g. oxidation and gas-water interaction) seem to represent the main controlling factor of reactive and/or water-soluble gas species, such as CH<sub>4</sub> and H<sub>2</sub>S. The total output of CO<sub>2</sub> from the abandoned stone quarry accounted for 0.53 % of total CO<sub>2</sub> discharged from the whole Colli Albani volcanic district. The naturally emitted toxic gases (e.g. CO<sub>2</sub>, H<sub>2</sub>S, CH<sub>4</sub>, GEM) largely affect the air quality and, as recorded in the past, are a threat for the human health in both the quarry and the nearby residential area. A mobile multi-instrumental station able to continuously and simultaneously acquire CO<sub>2</sub>, H<sub>2</sub>S, SO<sub>2</sub>, CH<sub>4</sub>, GEM and CO was deployed to verify the concentrations of both the main deep-originated gas compounds and potential secondary gaseous contaminants (i.e. SO<sub>2</sub>) throughout the urban settlement most exposed to the lethal gases. Hydrogen sulfide was found to be the most impacting gas, occasionally exceeding the 24-h air quality guideline for ambient air and causing odor annoyance among inhabitants at a distance up to more than 250 m downwind from the emitting area. Toxic gas accumulation up to hazardous levels was recognized in poorly ventilated basements, producing anomalous outdoor air concentrations at

1 the street level in front of the descending vehicular access to private garages even relatively far  
2 from the main emitting area. The geochemical survey carried out via the mobile multi-instrumental  
3 station and soil gas measurements resulted to be particularly efficient for evaluating the potential  
4 effects caused by gas emissions in inhabited areas and a pivotal tool for managing future urban  
5 development plans.  
6  
7  
8  
9  
10

11  
12 **Keywords:** *CO<sub>2</sub> diffuse degassing; air quality; Cava dei Selci; Colli Albani; gas hazard.*  
13  
14  
15  
16  
17  
18  
19

## 20 **1. Introduction**

21  
22

23 The Italian peninsula is characterized by intense and widespread CO<sub>2</sub>-rich gas venting, including  
24 both high-temperature gas discharges from the numerous active volcanic and hydrothermal systems,  
25 and low-temperature gas emissions from areas of quiescent volcanism and seismically active zones  
26 (Chiodini, 2008). Most gas manifestations occur in the peri-Tyrrhenian sector of central and  
27 southern Italy, i.e. southern Tuscany, northern Latium and Campania (Chiodini et al., 2000, 2004;  
28 Chiodini, 2008; Chiodini et al., 2013), where the large degassing is favored by (i) crustal thinning  
29 (<25 km; Scrocca et al., 2003), (ii) seismic activity (Frepoli and Amato, 1997; Mariucci et al., 1999;  
30 Chiodini et al., 2004 and references therein), (iii) high heat flow (up to 200 mW/m<sup>2</sup>; Cataldi et al.,  
31 1995) and (iv) Quaternary volcanism (i.e. a sequence of NW-SE aligned volcanic complexes,  
32 including Mt. Amiata, Latera, Vulsini, Cimino, Vico, Sabatini, Colli Albani; Mattei et al., 2010).  
33 Several discharging sites are located close to populated areas and the proximity of natural gas  
34 manifestations to residential settlements may cause severe environmental concerns, since they pose  
35 a serious risk for human health related to both short- and long-term exposure to toxic endogenous  
36 gases. The Colli Albani volcanic complex, located at about 20 km SE of Rome (Latium, Central  
37 Italy; Fig. 1a) and including some of the most densely populated municipalities of Latium, hosts a  
38 number of CO<sub>2</sub>-rich gas manifestations (e.g. Hooker et al., 1985; Giggenbach et al., 1988;  
39  
40  
41  
42  
43  
44  
45  
46  
47  
48  
49  
50  
51  
52  
53  
54  
55  
56  
57  
58  
59  
60  
61  
62  
63  
64  
65



1 Minissale, 2004; Carapezza et al., 2012). In this area, dissolved CO<sub>2</sub> in shallow ground waters may  
2 reach oversaturation, producing sudden and hazardous gas leakages at the surface (Chiodini and  
3 Frondini, 2001; Annunziatellis et al., 2003; Carapezza and Tarchini, 2007). The total CO<sub>2</sub>  
4 discharged from this volcanic district was estimated to be higher than  $4.2 \times 10^9$  mol/y over an area  
5 of about 1,500 km<sup>2</sup> (Chiodini and Frondini, 2001). One of the main degassing sites is located very  
6 close to the densely inhabited area of Cava dei Selci (Marino, Rome) (Fig. 1b), in an abandoned  
7 stone quarry at about 20 m from buildings and houses (Fig. 1c,d). Endogenous gases are discharged  
8 from punctual emissions and through diffuse soil degassing in such a huge amount that surrounding  
9 air occasionally becomes difficultly breathable up to even 2 m above the ground level (Pizzino et al.,  
10 2002; Carapezza et al., 2003 and references therein). The discharged gases mainly consist of CO<sub>2</sub>  
11 and H<sub>2</sub>S, which are denser than air and may accumulate in ground depressions and house basements  
12 (Annunziatellis et al., 2003; Beaubien et al., 2003; Carapezza et al., 2003, 2012). Displacing  
13 oxygen, CO<sub>2</sub> can cause severe health effects on humans and animals (e.g. rapid breathing and heart  
14 rate, headache, nausea and vomiting, collapse, convulsions, and even coma and death) when present  
15 at high concentrations (Gellhorn, 1936; Sechzer et al., 1960; Langford, 2005). The immediately  
16 dangerous to life or health (IDLH) value established by the National Institute for Occupational  
17 Safety and Health (NIOSH) is of 72,000 mg/m<sup>3</sup> (NIOSH, 1996; Department of Health and Human  
18 Services (NIOSH), 2007). Consequently, few minutes of exposure at 126,000-180,000 mg/m<sup>3</sup>  
19 produce unconsciousness (NIOSH, 1996). Hydrogen sulfide levels above 450 mg/m<sup>3</sup> cause, in order  
20 of increasing concentration, pulmonary edema, strong central nervous system stimulation,  
21 hyperpnoea followed by respiratory arrest, immediate collapse with respiration paralysis (WHO,  
22 2000). The lowest-observed-adverse-effect level (LOAEL) of H<sub>2</sub>S is 15 mg/m<sup>3</sup>, when eye irritation  
23 occurs, although a lower threshold (2.8 mg/m<sup>3</sup>) was recognized for respiratory effects in asthmatics  
24 (WHO, 2003 and references therein). Moreover, hazardous concentrations of other toxic species in  
25 the gases discharged from Cava dei Selci were also recognized. For instance, anomalously high  
26 concentrations of Rn in soil gases from the Colli Albani area were recorded, with contents >100  
27

1 kBq/m<sup>3</sup> near the town of Cava dei Selci (Beaubien et al., 2003), exposing inhabitants to a long-term  
2 risk of developing lung cancer (Dubois, 2005).  
3

4 In such a context, the adoption of a proper methodological approach for the characterization of gas  
5 emissions and the estimation of their impact on air quality is pivotal for a correct assessment of the  
6 hazard to human health and the definition of intervention plans. This approach is expected to  
7 answer two crucial questions:  
8  
9

- 10 – which is the total output of the released endogenous gases?  
11
- 12 – which is the effective impact of these emissions on the air quality in the surroundings of the  
13 discharging area?  
14  
15  
16  
17  
18  
19  
20

21 Gases discharged to the atmosphere through punctual gas vents or soil degassing can be modified  
22 by chemical-physical processes (e.g. oxidation reactions, vapor condensation, interactions with  
23 shallow aquifers; e.g. Tassi et al., 2013) able to affect, for example, reduced and/or highly soluble  
24 species (e.g. H<sub>2</sub>S and CH<sub>4</sub>). Similarly, secondary processes driven by microorganisms (Bacteria and  
25 Archaea), inhabiting terrains at shallow depth, are expected to play an important role as they can  
26 alter the original composition of interstitial soil gases (e.g. Huber et al., 2000; Norris et al., 2002;  
27 Glamoclija et al., 2004; Henson et al., 2005; D'Alessandro et al., 2011; Gagliano et al., 2014; Tassi  
28 et al., 2015a,b). Hence, this implies that inorganic and organic processes have to be taken into  
29 account for a correct assessment of the poisoning gases emitted from the anomalous degassing  
30 systems (e.g. Chiodini et al., 2005, 2010). Moreover, the dispersion of deep-originated gases in the  
31 air is dependent on several variables such as: (i) the output rate from the emitting source(s), (ii)  
32 meteorological parameters (e.g. wind speed and direction, air humidity and temperature), (iii)  
33 physical properties of each gas species (e.g. gas molecular weight), and (iv) chemical reactions in  
34 air affecting the different gas species at a various degree as a function of their reactivity. Such a  
35 high number of parameters makes difficult to define the correct positioning of a fixed measurement  
36 station that is the classical approach adopted to monitor an area affected by air contamination (e.g.  
37 Peralta et al., 2013; Olafsdottir et al., 2014). Consequently, mobile measurement platforms (e.g.  
38  
39  
40  
41  
42  
43  
44  
45  
46  
47  
48  
49  
50  
51  
52  
53  
54  
55  
56  
57  
58  
59  
60  
61  
62  
63  
64  
65

1 Kolb et al., 2004), able to provide a large dataset of air pollutants along pathways within and in the  
2 immediate surroundings of the study area can successfully be applied to obtain information about  
3  
4 the role played by the environmental parameters and chemical processes on air quality (Cabassi et  
5 al., 2017 and references therein). The final target of this strategy is that to recognize the prone areas  
6  
7 to hazardous gases and the best sites where to locate fixed measuring stations.  
8  
9

10  
11 This paper reports the data of (i) chemical composition of endogenous gases emitted from punctual  
12 discharges and permeating the soil at shallow depths, (ii) soil CO<sub>2</sub>, H<sub>2</sub>S and CH<sub>4</sub> fluxes from the  
13 abandoned stone quarry, and (iii) concentrations of CO<sub>2</sub>, H<sub>2</sub>S, SO<sub>2</sub>, CH<sub>4</sub>, GEM and CO in air in the  
14 abandoned stone quarry and in the nearby residential area, obtained during a field survey carried out  
15  
16 at Cava dei Selci from 5 to 6 April 2016. The main aims were to (i) chemically and isotopically  
17 characterize the gases discharged from such anomalous degassing area, (ii) estimate their effective  
18 impact on air quality in this densely populated area, and (iii) furnish a new and most complete  
19 dataset of the Cava de Selci natural gas emissions.  
20  
21  
22  
23  
24  
25  
26  
27  
28  
29  
30

## 31 **2. Study area**

32  
33  
34  
35  
36 Cava dei Selci is an intensely urbanized area in the municipality of Marino (ca. 43,500 inhabitants),  
37 close to the Ciampino International Airport (Rome, central Italy). It is located on the NW side of  
38 Colli Albani (Fig. 1a,b), a quiescent alkali-potassic volcanic district (Trigila et al., 1995; Peccerillo,  
39 1999, 2005; Giordano et al., 2006; Carapezza et al., 2010) characterized by a low-to-medium-  
40 enthalpy CO<sub>2</sub>-rich fluid reservoir (Giggenbach et al., 1988) that is part of a regional aquifer (e.g.  
41 Chiodini et al., 1999) hosted in the structural highs of the Mesozoic carbonates overlying a  
42 Paleozoic metamorphic basement (e.g. Orlando et al., 1994). The origin of CO<sub>2</sub> was ascribed to (i)  
43 metamorphic reactions involving carbonate formations and (ii) mantle degassing (Giggenbach et al.,  
44 1988; Rogie et al., 2000; Chiodini and Frondini, 2001; Minissale, 2004; Carapezza and Tarchini,  
45 2007; Iacono Marziano et al., 2007). Nitrogen, H<sub>2</sub>S and CH<sub>4</sub> are minor constituents of the gases  
46 emitted from the area (Annunziatellis et al., 2003; Chiodini and Frondini, 2001; Carapezza et al.,  
47  
48  
49  
50  
51  
52  
53  
54  
55  
56  
57  
58  
59  
60  
61

1 2003), as well as the short-lived Rn, whose presence suggests that fluids rise quite rapidly through  
2 high permeable pathways, i.e. faults and fractures (Beaubien et al., 2003). Actually, Cava dei Selci  
3  
4 lies on the north-western margin of the NE volcanotectonic active structure bordering the Ciampino  
5  
6 horst, a NW-SE oriented structural high of the Mesozoic carbonate basement (Amato and  
7  
8 Chiarabba, 1995; Di Filippo and Toro, 1995; Carapezza et al., 2003), where is located one of the  
9  
10 main degassing sites of the Colli Albani volcanic complex. It consists of a 10,000 m<sup>2</sup> wide area  
11  
12 located close to residential buildings (Fig. 1c,d). Until the 1970s, the site was a stone quarry. The  
13  
14 excavation removed the superficial low permeability volcano-sedimentary cover and formed a  
15  
16 depression that was filled with loose material after the closure of the quarry. The highly permeable  
17  
18 filling deposits were progressively altered by the uprising acidic fluids, and turned to be clay-rich  
19  
20 (Carapezza et al., 2003; Carapezza and Tarchini, 2007; Carapezza et al., 2012). A stagnant water  
21  
22 pool emerges at the bottom of the depression during the rainy season (November to March) and  
23  
24 disappears in the summer period (June to September). The gas is released either diffusively from the  
25  
26 soil or through punctual vents, the latter forming bubbling pools in the rainy season (Carapezza et  
27  
28 al., 2003). Moreover, less than 200 m north of the degassing area, a dry gas emitting old water well  
29  
30 (Fig. 1c,e) is present where a gas blast likely occurred in the recent past as happened for other wells  
31  
32 in the region (Carapezza and Tarchini, 2007; Carapezza et al., 2010).  
33  
34  
35  
36  
37  
38  
39  
40

41 In the abandoned quarry, lethal concentrations of both CO<sub>2</sub> and H<sub>2</sub>S were occasionally measured in  
42  
43 previous surveys (Carapezza et al., 2010, 2012) at ≤1 m height above the ground, particularly at  
44  
45 dawn when wind ceases to blow. Accordingly, several lethal accidents caused by gas inhalation  
46  
47 occurred in the area, involving both humans (a man died in December 2000) and animals (29 cows  
48  
49 in 1999, a sheep in March 2000 and 3 sheep in 2001 were asphyxiated; Annunziatellis et al., 2003;  
50  
51 Carapezza et al., 2003). An exhaustive solution to the problem is far from being achieved by risk  
52  
53 stakeholders, notwithstanding the insistent recommendations based on outdoor and indoor  
54  
55 measurements of toxic gases, clearly highlighting the strong risks posed by these natural gas  
56  
57 emissions (e.g. Beaubien et al., 2003; Carapezza et al., 2003, 2010, 2012). After the installation of a  
58  
59  
60  
61  
62  
63  
64  
65

1 CO<sub>2</sub> measurement station that was prematurely dismissed, the main emission zone, i.e. the old  
2 quarry, was only temporary fenced with some wire mesh.  
3  
4

### 5 **3. Materials and Methods**

#### 6 **3.1 Sampling and analytical methods for gases**

##### 7 **3.1.1 Sampling procedures**

8  
9  
10  
11  
12  
13  
14  
15  
16 Gases from two gas emissions (G1 and G2; Fig. 1f) and from the gas-blowing well (G3) (Fig. 1c,e)  
17 were collected into (i) two-way Pyrex bottles, for the analysis of the <sup>13</sup>C/<sup>12</sup>C ratios of CO<sub>2</sub> and CH<sub>4</sub>  
18 and the isotope compositions of He and Ar, (ii) pre-evacuated 60 cc glass flasks, equipped with  
19 Teflon stopcocks and filled with 20 mL of a 4 M NaOH solution, for determination of the chemical  
20 composition (Vaselli et al., 2006) and (iii) 30 mL glass bottles equipped with two stopcocks each.  
21 At each sampling point, a third aliquot for the analysis of the organic gases was collected into a 12  
22 cc glass vial equipped with a pierceable rubber septum (Labco Exetainer<sup>®</sup>) (Tassi et al., 2015a).  
23  
24  
25  
26  
27  
28  
29  
30  
31  
32

33 Interstitial soil gases were collected in 35 sites in the abandoned stone quarry (Fig. 1f) using 12 cc  
34 glass vials and a 1 m long stainless steel tube (Tassi et al., 2015a) inserted at 20 or 10 cm depth  
35 where either the shallowness of the water table or the soil hardness did not allowed to reach higher  
36 depths.  
37  
38  
39  
40  
41  
42  
43

##### 44 **3.1.2 Analytical techniques**

45  
46  
47 Inorganic gases in both the headspace of the 60 cc glass flasks (N<sub>2</sub>, O<sub>2</sub>+ Ar, Ne, and He) and the 12  
48 cc glass vials (N<sub>2</sub>, O<sub>2</sub>+Ar) were analyzed using a Shimadzu 15A gas chromatograph (GC) equipped  
49 with a thermal conductivity detector (TCD) and a 10 m long 5A Molecular Sieve column and He or  
50 Ar as gas carrier. Carbon dioxide and H<sub>2</sub>S in the glass vials were analyzed using the same GC  
51 equipped with a 3 m long column packed with Porapak Q 80/100 mesh and He as gas carrier. Argon  
52 and O<sub>2</sub> peaks were efficiently separated using a Thermo Focus gas chromatograph equipped with a  
53  
54  
55  
56  
57  
58  
59  
60  
61  
62  
63  
64  
65

1  
2  
3  
4  
5  
6  
7  
8  
9  
10  
11  
12  
13  
14  
15  
16  
17  
18  
19  
20  
21  
22  
23  
24  
25  
26  
27  
28  
29  
30  
31  
32  
33  
34  
35  
36  
37  
38  
39  
40  
41  
42  
43  
44  
45  
46  
47  
48  
49  
50  
51  
52  
53  
54  
55  
56  
57  
58  
59  
60  
61  
62  
63  
64  
65

30 m long capillary molecular sieve column and a TCD. Hydrogen and CO were measured in 30 ml glass bottles using a Carlo Erba GC, equipped with a Reductant Gas Detector (RGD) and 5m long 5A Molecular Sieve packed column.

The alkaline solution in the glass flasks was used for the analysis of (i) CO<sub>2</sub>, as CO<sub>3</sub><sup>2-</sup> by acidimetric titration (AT) with 0.5 N HCl solution, and (ii) H<sub>2</sub>S, as SO<sub>4</sub><sup>2-</sup> by ion chromatography (IC) after oxidation using H<sub>2</sub>O<sub>2</sub> (Montegrossi et al., 2001; Vaselli et al., 2006).

Light hydrocarbons (C<sub>≤3</sub>) were analyzed using a Shimadzu 14A gas chromatograph equipped with a Flame Ionization Detector (FID) and a 10 m long stainless steel column packed with Chromosorb PAW 80/100 mesh coated with 23 % SP 1700. The heavier Volatile Organic Compounds (VOCs) were analyzed by GC (Thermo Trace Ultra) coupled to a Thermo DSQ Quadrupole Mass Spectrometer (MS) after extraction using the Solid Phase Micro Extraction (SPME; Arthur and Pawliszyn, 1990) technique. The SPME was carried out using a 2 cm long three-phase fiber made of DiVinylBenzene (DVB) – Carboxen (Car) – PolyDiMethylSiloxane (PDMS) (Supelco; Bellefonte, PA, USA). In the laboratory, the fiber was introduced into the glass vials through the porous membrane using a manual SPME device and exposed to the sampled gases for 30 min at 20 °C. Then, the VOCs absorbed into the SPME fiber were desorbed for 2 min at 230 °C in the column headspace of the GC-MS. The desorbed gases were injected through a port operating in splitless mode and equipped with a SPME liner (0.75 mm inner diameter) into a 30 m × 0.25 mm (1.4 μm inner diameter) film thickness TR-V1 fused silica capillary column (Thermo), using He as carrier gas at a flow rate of 1.3 mL/min in constant pressure mode. The column oven temperature was set, as follows: 35 °C (hold 10 min), ramp at 5.5 °C/min to 180 °C (hold 3 min), ramp at 20 °C/min up to 230 °C (hold 6 min). After the chromatographic separation, gases passed through a transfer-line set at 230 °C to the MS operating in positive electron impact mode (EI), with an ionization energy of 70 eV and a source temperature of 250 °C. A mass range from 35 to 400 m/z in full scan mode was analyzed. Retention times of the chromatographic peaks and the mass spectra were both used to identify VOCs detected by the quadrupole detector, using the mass spectra database of the NIST05

1 library (NIST, 2005) for comparison. Quantitative analyses were carried out by external standard  
2 calibration procedure using Accustandard<sup>®</sup> mixtures in methanol or, alternatively, hexane solvent.  
3  
4 Relative Standard Deviation (RSD), calculated from five replicate analyses of the standard  
5 mixtures, was <5%. The limit of quantification (LOQ) was determined by linear extrapolation from  
6  
7 the lowest standard in the calibration curve using the area of a peak having a signal/noise ratio of 5.  
8  
9 Analytical errors for GC, AT and IC were <5%.  
10  
11

12  
13 The gas samples destined for noble gas isotopic analyses were purified in high-vacuum line with  
14 cryogenic traps (10 K) directly connected to the mass spectrometer. The <sup>3</sup>He/<sup>4</sup>He ratios were  
15 measured by a Helix SFT-GVI double collector and <sup>40</sup>Ar, <sup>38</sup>Ar, e <sup>36</sup>Ar by a Helix MC-GVI mass  
16 spectrometer. Calibration for measurements of isotope abundances of He and Ar were performed  
17 using atmospheric standards. The analytical errors for He and Ar isotope analyses were ≤0.3 % and  
18 ≤0.1 %, respectively.  
19  
20

21  
22 The <sup>13</sup>C/<sup>12</sup>C ratios of CO<sub>2</sub> (expressed in ‰ vs. V-PDB) were measured with a Thermo Delta V Plus  
23 dual inlet mass spectrometer after purification of the gas mixture by standard procedures using  
24 cryogenic traps (Evans et al., 1998; Vaselli et al., 2006; Paonita et al., 2012). Calibration was  
25 performed by using a standard prepared by quantitative reaction of certified Carrara Marble  
26 (δ<sup>13</sup>C<sub>MAB</sub> = +2.45 ‰ vs. V-PDB) with anhydrous phosphoric acid (H<sub>3</sub>PO<sub>4</sub>).  
27  
28

29  
30 The isotopic analysis <sup>13</sup>C/<sup>12</sup>C of CH<sub>4</sub> were performed by using a Delta Plus XP IRMS equipped  
31 with a Thermo TRACE GC interfaced with Thermo GC/C III. Thermo TRACE gas chromatograph  
32 was equipped with a Poraplot-Q column. The injection system is better described in Grassa et al.,  
33 (2010). CH<sub>4</sub> was quantitatively converted to CO<sub>2</sub> by passing through a combustion oven (T=940  
34 °C). The <sup>13</sup>C/<sup>12</sup>C ratios are reported as δ<sup>13</sup>C values against V-PDB standard. The uncertainties of  
35 measurements are ±0.15‰.  
36  
37  
38  
39  
40

### 41 **3.2 Soil flux measurements**

42  
43  
44  
45  
46  
47  
48  
49  
50  
51  
52  
53  
54  
55  
56  
57  
58  
59  
60  
61  
62  
63  
64  
65

1 Soil fluxes of CO<sub>2</sub>, CH<sub>4</sub> and H<sub>2</sub>S were measured at 81 sites throughout the abandoned stone quarry  
2 using the “accumulation chamber” (AC) method (Chiodini et al., 1998). The measurements were  
3  
4 performed using West Systems Co. Ltd portable flux meters, consisting of (i) an inverted chamber  
5  
6 (a cylindrical metal vase with a basal area of 200 cm<sup>2</sup> and an inner volume of 3,060 cm<sup>3</sup>), (ii) CO<sub>2</sub>,  
7  
8 CH<sub>4</sub> or H<sub>2</sub>S gas detectors, (iii) an analog-to-digital (AD) converter, and (iv) a palmtop computer.  
9  
10 The AC detectors consist of (i) an Infra-Red (IR) spectrophotometer (Licor<sup>®</sup> Li-820, measurement  
11  
12 range and accuracy: 0-36,000 mg/m<sup>3</sup> and 4%, respectively) for CO<sub>2</sub>, (ii) a detector based on tunable  
13  
14 diode laser absorption spectroscopy (TDLAS) combined with a Herriot multipass cell for CH<sub>4</sub>, and  
15  
16 (ii) an electrochemical detector for H<sub>2</sub>S. Once the chamber was firmly placed on the ground, the soil  
17  
18 gas was continuously pumped from the chamber, using a low-flux pump (20 mL/s), to the IR  
19  
20 spectrophotometer, and then injected back into the chamber to minimize the disturbance on the gas  
21  
22 flux. Close to initial conditions, if CO<sub>2</sub> concentration in the soil is much higher than CO<sub>2</sub>  
23  
24 concentration in air, the increase in time of the gas concentrations inside the chamber (dC<sub>i</sub>/dt) is  
25  
26 proportional to the gas flux from the soil (Φ<sub>i</sub>), according to the following equation (Chiodini, 1998):  
27  
28  
29  
30  
31  
32

$$\phi_i = cf \times dC_i/dt \quad (1)$$

33  
34 where *i* is CO<sub>2</sub>, CH<sub>4</sub> or H<sub>2</sub>S, while *cf* is the proportionality factor between dC<sub>i</sub>/dt and Φ<sub>i</sub>, which  
35  
36 depends on the geometry of the measuring equipment (Chiodini, 1998). The lower detection limits  
37  
38 (d.l.) for ΦCO<sub>2</sub>, ΦCH<sub>4</sub> and ΦH<sub>2</sub>S were ~0.08, ~0.008 and ~0.00348 g m<sup>-2</sup> day<sup>-1</sup>, respectively. For  
39  
40 statistical analysis, values below the d.l. were replace by d.l./2.  
41  
42  
43  
44  
45

46 The probability distribution analysis of flux data and the estimation of the total CO<sub>2</sub>, CH<sub>4</sub> and H<sub>2</sub>S  
47  
48 output from the study area was performed through the graphical statistical approach (GSA) method  
49  
50 described by Chiodini et al. (1998), while the sequential Gaussian simulations (sGs) approach was  
51  
52 applied in order to produce a map of CO<sub>2</sub> diffuse degassing (Deutsch and Journel, 1998; Cardellini  
53  
54 et al., 2003; Frondini et al., 2004; Cardellini et al., 2017).  
55  
56  
57  
58

### 59 **3.3 Measurements of air pollutants**



1  
2 Air pollutants were determined (i) at two sites, located within the abandoned stone quarry in Cava  
3 dei Selci (F1; Fig. 1f) and in close proximity to the gas-blowing well (F2; Fig. 1c,e), respectively,  
4 and (ii) along the streets of Cava dei Selci and inside two private garages (Fig. 1g) using a Mobile  
5 Multi-instrumental Station (MMS). The location of the fixed stations and the measuring pathways  
6 throughout the town were digitalized using a portable GPS (Garmin® GPSMAP 62), whilst the  
7 meteorological parameters (wind speed and direction) were measured with a Davis® Vantage Vue  
8 weather mobile station placed within the study area. The measured air pollutants were, as follows:  
9 CO<sub>2</sub>, H<sub>2</sub>S, SO<sub>2</sub> and GEM (Gaseous Elemental Mercury). The  $\delta^{13}\text{C-CO}_2$  values at the fixed stations  
10 and the concentrations of CO and CH<sub>4</sub> via the mobile station were also measured.  
11  
12  
13  
14  
15  
16  
17  
18  
19  
20  
21  
22

### 23 **3.3.1 Fixed measuring stations**

24  
25 At F1 and F2 the measurements were performed at 1 and 0.25 m above the ground, respectively.  
26  
27 The instruments were placed downwind of the emitting area and the gas-blowing well, respectively.  
28  
29 The air concentrations of sulfur-bearing inorganic gases (H<sub>2</sub>S and SO<sub>2</sub>) were determined by using a  
30 Thermo® 450i analyzer featuring a pulsed fluorescence technology. The air is pumped at 1 L/min  
31 into the analyzer and directed to either (i) a converter, where H<sub>2</sub>S is oxidized to SO<sub>2</sub> (efficiency >80  
32 %) or (ii) the fluorescence chamber, i.e. bypassing the converter. In the fluorescence chamber,  
33 pulsating UV light excites the SO<sub>2</sub> molecules. As the excited SO<sub>2</sub> molecules decay to lower energy  
34 states, they emit a UV light, detected by a photomultiplier tube (PMT), whose intensity is  
35 proportional to the SO<sub>2</sub> concentration. When the air sample passes through the converter, the  
36 instrument measures the concentrations of Combined Sulfur (CS), i.e. the sum of SO<sub>2</sub> and H<sub>2</sub>S.  
37  
38 When the air flux bypasses the converter, the analyzer only determines SO<sub>2</sub>. The H<sub>2</sub>S content is  
39 then calculated as the difference between the two signals (Thermo Fisher Scientific, 2012). The  
40 instrument provides concentrations by averaging the measurements carried out each 60s (precision  
41  $\pm 1\%$ ; Thermo Fisher Scientific, 2012), by averaging the 60 s measurements (linearity  $\pm 1\%$ ;  
42 Thermo Fisher Scientific, 2012). The detection limits are 5.2 and 2.8  $\mu\text{g}/\text{m}^3$  for SO<sub>2</sub> and H<sub>2</sub>S,  
43  
44  
45  
46  
47  
48  
49  
50  
51  
52  
53  
54  
55  
56  
57  
58  
59  
60  
61  
62  
63  
64  
65

1  
2  
3  
4  
5  
6  
7  
8  
9  
10  
11  
12  
13  
14  
15  
16  
17  
18  
19  
20  
21  
22  
23  
24  
25  
26  
27  
28  
29  
30  
31  
32  
33  
34  
35  
36  
37  
38  
39  
40  
41  
42  
43  
44  
45  
46  
47  
48  
49  
50  
51  
52  
53  
54  
55  
56  
57  
58  
59  
60  
61  
62  
63  
64  
65

respectively (Thermo Fisher Scientific, 2012). During the field surveys, the instrumentation was power-supplied by a high-performance portable gel battery.

GEM air concentration measurements were performed by using a Lumex® RA-915M analyzer, i.e. a portable atomic absorption spectrometer with Zeeman background correction for interference-free measurements combined with high frequency modulation of polarized light. The radiation source (Hg lamp) is placed in a permanent magnetic field, whereby the 254 nm mercury resonance line is split into three polarized components, two of which are detected for the analysis. After passing through a polarization modulator, the radiation reaches a multi-path cell that isolates the 254 nm resonance line allowing high selectivity and sensitivity (Sholupov and Ganeyev, 1995; Sholupov et al., 2004). The instrument operates at a flow rate of 10 L/min and is supplied by a rechargeable internal battery allows up to 8 h of continuous measurements. The detection limit is 2 ng/m<sup>3</sup> while the accuracy of the method is 20% from 2 to 50,000 ng/m<sup>3</sup> (Sholupov and Ganeyev, 1995; Sholupov et al., 2004). For the present study, the measurement acquisition frequency was of 1 s and GEM data were averaged over 1 min to be coupled with those of H<sub>2</sub>S and SO<sub>2</sub>.

The concentrations and isotopic composition of CO<sub>2</sub> in air were measured by using a Thermo Scientific Delta Ray™ Isotope Ratio Infrared Spectrometer (IRIS) analyzer. The instrument is equipped with a tunable diode laser operating at a mid-infrared wavelength (4.3 μm) employing a simple and direct absorption approach using a path length of only 5 m. The analyzer works at ambient CO<sub>2</sub> over the concentration range of 360–6,300 mg/m<sup>3</sup> and high precision is achieved using gas standard for calibration at known CO<sub>2</sub> concentration and isotope composition every 20 minutes. The sampling frequency of the detector signal is recorded at 1 Hz, and the δ<sup>13</sup>C<sub>(CO<sub>2</sub>)</sub> values are averaged over a time interval of 60 seconds of stable acquisition.

The isotope composition of carbon is reported as δ<sup>13</sup>C-CO<sub>2</sub> values expressed in ‰ versus V-PDB international standard. The adopted measurement method allows achieving precision for δ<sup>13</sup>C<sub>(CO<sub>2</sub>)</sub> of ± 0.15 ‰ (Di Martino et al., 2016).

1 Sampling point was placed at approximately 30 m away from the main degassing area and 0.75 m  
2 above the ground.  
3

### 4 **3.3.2 Mobile multi-instrumental station (MMS)**

5  
6  
7 The MMS is a prototype developed by West Systems Ltd (Laville et al., 2015) for the real-time  
8  
9 continuous monitoring of air quality. The traction system (Fig. 1g) includes a self-propelled crawler  
10  
11 machine equipped with two engines and the respective electronic controllers. The battery pack of  
12  
13 the crawler machine, coupled with an inverter of 24 VDC input, provides AC (alternating current)  
14  
15 power (up to 1,500 W) for the instruments (Laville et al., 2015).  
16  
17

18  
19 The gas analyzers set on the MMS was composed by 4 modules, as follows: (i) Thermo® 450i  
20  
21 analyzer, (ii) Lumex® RA-915M analyzer, (iii) Los Gatos Research Ultraportable Greenhouse Gas  
22  
23 Analyzer (LGR-UGGA) for CO<sub>2</sub> and CH<sub>4</sub>, and (iv) Los Gatos Research LGR 913-0015 analyzer for  
24  
25 CO.  
26  
27

28  
29 The LGR UGGA and LGR 913-0015 gas analyzers are spectrometers using Los Gatos Research's  
30  
31 patented off-axis ICOS (integrated cavity output spectroscopy) technology, a fourth generation  
32  
33 cavity. They require 60 W (powered with 10-30 VDC) and 300 W (powered with 230 VAC),  
34  
35 respectively. The measurement range of LGR UGGA is from 1 to 36,000 mg/m<sup>3</sup> and from 0.007 to  
36  
37 66 mg/m<sup>3</sup> for CO<sub>2</sub> and CH<sub>4</sub>, respectively, whilst the linear dynamic range of LGR 913-0015 is from  
38  
39 0.006 to 4.58 mg/m<sup>3</sup>.  
40  
41  
42  
43

## 44 **4. Results**

### 45 **4.1 Chemical and isotopic ( $\delta^{13}\text{C-CO}_2$ , $^{40}\text{Ar}/^{36}\text{Ar}$ and $R_c/R_a$ ) composition of gas emissions**

46  
47  
48 The chemical and isotopic composition of gases emitted from (i) the two punctual vents (G1 and  
49  
50 G2; Fig. 1f) and (ii) the gas-blowing well (G3; Fig. 1c,e) are reported in Table 1. The chemical  
51  
52 composition of the inorganic gas fraction was largely dominated by CO<sub>2</sub> (with concentrations  
53  
54 ranging from 982 to 990 mmol/mol), with H<sub>2</sub>S as the second most abundant constituent (from 5.6 to  
55  
56  
57  
58  
59  
60  
61  
62  
63  
64  
65

11 mmol/mol). The concentrations of N<sub>2</sub> varied from 3.2 to 5.6 mmol/mol, whilst O<sub>2</sub> and Ar ranged from 0.087 to 0.13 and from 0.026 to 0.051 mmol/mol, respectively. Methane had concentrations between 0.68 to 0.91 mmol/mol, whilst H<sub>2</sub> and CO ranged from 0.015 to 0.056 and from 0.0009 to 0.0033 mmol/mol, respectively. Helium and Ne were up to 0.0011 and 0.000078 mmol/mol, respectively.

The total content of VOCs ranged from 10.8 to 12.4 μmol/mol (Table 1). Alkanes were the most abundant species, with concentrations ranging from 4.0 to 5.3 μmol/mol, corresponding to 35-45 % of the total organic fraction (ΣVOCs). The concentrations of ethane (C<sub>2</sub>H<sub>6</sub>, from 2.5 to 3.6 μmol/mol) were one order of magnitude higher than those of propane (C<sub>3</sub>H<sub>8</sub>, ≤0.66 μmol/mol), normal-butane (n-C<sub>4</sub>H<sub>10</sub>, ≤0.25 μmol/mol) and iso-butane (i-C<sub>4</sub>H<sub>10</sub>, ≤0.21 μmol/mol) and long-chain C<sub>5+</sub> alkanes (≤0.71 μmol/mol). S-substituted compounds were relatively abundant, ranging from 1.7 to 3.9 μmol/mol (i.e. from 16 to 35 %ΣVOCs). O-bearing species included esters+acids (from 1.8 to 2.4 μmol/mol), ketones (from 0.15 to 0.60 μmol/mol) and aldehydes (from 0.11 to 0.15 μmol/mol), corresponding to 19 up to 25 % of the organic gas fraction. Among aromatics, C<sub>6</sub>H<sub>6</sub> was the most abundant (from 0.47 to 0.64 μmol/mol) species, while the concentrations of branched aromatics ranged from 0.61 to 0.78 μmol/mol. On the whole, aromatics added up to 10-12 % ΣVOCs).

The δ<sup>13</sup>C-CO<sub>2</sub> and δ<sup>13</sup>C-CH<sub>4</sub> values ranged from 0.73 to 1.08 ‰ vs. V-PDB and from -32 to -29 ‰ vs. V-PDB, respectively (Table 1). These δ<sup>13</sup>C-CO<sub>2</sub> values are similar to those previously reported for gases collected from this area (Giggenbach et al., 1988; Chiodini and Frondini, 2001; Annunziatellis et al., 2003; Carapezza and Tarchini, 2007; Carapezza et al., 2012).

The <sup>40</sup>Ar/<sup>36</sup>Ar ratios varied from 293 to 299 (Table 1), basically consisting with that of air. The measured isotopic composition of He was expressed as R/R<sub>a</sub>, where R refers to the <sup>3</sup>He/<sup>4</sup>He ratio in the sample and R<sub>a</sub> is the <sup>3</sup>He/<sup>4</sup>He ratio in the air (i.e. 1.4 × 10<sup>-6</sup>). The measured R/R<sub>a</sub> values (Table 1) were corrected for air contamination by using the He/Ne ratio, as follows:

$$R_c/R_a = \frac{(R/R_a)(\text{He/Ne})_m - (\text{He/Ne})_a}{(\text{He/Ne})_m - (\text{He/Ne})_a} \quad (2)$$

where subscripts  $m$  and  $a$  refer to the values measured in samples and in air, respectively. The corrected  $R_c/R_a$  ratios were 1.41 in both G1 and G3 samples (Table 1).

#### 4.2 Chemical composition of interstitial soil gases

The chemical composition of the interstitial soil gases is reported in Table 2. Carbon dioxide and  $N_2$  displayed highly variable and inversely correlated concentrations, ranging from 4.9 to 962 mmol/mol and from 36 to 671 mmol/mol, respectively. On the basis of the  $CO_2/N_2$  ratio, three groups of interstitial soil gases were distinguished, as follows: (i) group A, characterized by a chemical composition largely dominated by  $CO_2$ , with  $CO_2/N_2$  ratios higher than 10 and up to 27, (ii) group B, with  $CO_2/N_2$  ratios ranging from 1.28 to 9.53, and (iii) group C, with a  $N_2$ -dominated composition and  $CO_2/N_2$  ratios  $\leq 0.62$ .

Group A soil gases were characterized by relevant concentrations of  $CO_2$  ( $\geq 900$  mmol/mol),  $H_2S$  (from 0.06 to 3.30 mmol/mol) and  $CH_4$  (from 0.02 to 0.13 mmol/mol). Nitrogen,  $O_2$  and Ar ranged from 36 to 89 mmol/mol, 0.51 to 12 mmol/mol and from 0.85 to 2.20 mmol/mol, respectively.

Similarly to A soil gases, group B interstitial soil gases were dominated by  $CO_2$  ( $\leq 896$  mmol/mol).

On average, lower concentrations of  $H_2S$  and  $CH_4$  relative to those measured in the A soil gases were also detected (ranging from 0.06 to 2.10 mmol/mol and from 0.01 to 0.12 mmol/mol), whereas  $N_2$ ,  $O_2$  and Ar were recovered at higher amounts (from 94 to 395 mmol/mol, from 5.10 to 104 mmol/mol and from 2.30 to 9.90 mmol/mol, respectively).

Group C soil gases, showing  $N_2$ ,  $O_2$  and Ar concentrations  $\geq 484$ ,  $\geq 136$  and  $\geq 11$  mmol/mol, respectively, had  $CO_2$  and  $CH_4$  concentrations  $\leq 302$  and  $\leq 0.03$  mmol/mol, respectively, whereas  $H_2S$  was below the detection limits.

The total content of VOCs ( $\Sigma$ VOCs), ranging from 0.05 to 1.15  $\mu$ mol/mol, increased with the  $CO_2/N_2$  ratio, the highest and lowest concentrations being generally measured in the groups A

( $\Sigma\text{VOCs} \geq 0.15 \mu\text{mol/mol}$ ) and *C* ( $\Sigma\text{VOCs} \leq 0.13 \mu\text{mol/mol}$ ). The organic fraction was largely dominated by alkanes (ranging from 73 to 97 % with respect to the  $\Sigma\text{VOCs}$ ), mainly consisting of ethane (up to  $0.61 \mu\text{mol/mol}$ ) and propane (up to  $0.15 \mu\text{mol/mol}$ ), with minor amounts of iso-butane (up to  $0.026 \mu\text{mol/mol}$ ), normal-butane (up to  $0.015 \mu\text{mol/mol}$ ) and  $\text{C}_{5+}$  alkanes (up to  $0.16 \mu\text{mol/mol}$ ). The relative abundances of alkanes generally increased as the  $\text{CO}_2/\text{N}_2$  ratio decreased, with values ranging from 82 to 91 % $\Sigma\text{VOCs}$ , from 73 to 97 % $\Sigma\text{VOCs}$ , and from 85 to 96 % $\Sigma\text{VOCs}$  in groups *A*, *B* and *C*, respectively (Fig. 2). Moreover, S-bearing compounds were detected almost exclusively in the *A* soil gases ( $\leq 0.3$  % $\Sigma\text{VOCs}$  and up to  $0.0012 \mu\text{mol/mol}$ ), being only occasionally recovered in *B* soil gases ( $\leq 0.2$  % $\Sigma\text{VOCs}$  and up to  $0.0009 \mu\text{mol/mol}$ ). Alkenes showed an opposite trend with respect to alkanes, ranging from 3.9 to 11.8 % $\Sigma\text{VOCs}$  in *A* soil gases (i.e. from  $0.009$  to  $0.110 \mu\text{mol/mol}$ ) to  $\leq 8.7$  % $\Sigma\text{VOCs}$  (i.e.  $\leq 0.011 \mu\text{mol/mol}$ ) in *C* soil gases (Fig. 2). The relative abundances of aromatic and cyclic compounds displayed no clear trend among the analyzed soil gases, ranging from 0.2 to 2.4 % $\Sigma\text{VOCs}$  and from 0.5 to 2.5 % $\Sigma\text{VOCs}$ , respectively. The concentrations of aromatic and cyclic compounds were comparable in groups *A* and *B* ( $\leq 0.013$  and  $\leq 0.012 \mu\text{mol/mol}$ , respectively), whereas lower values were measured in *C* soil gases ( $\leq 0.0015$  and  $\leq 0.0018 \mu\text{mol/mol}$ , respectively). Differently, O-bearing compounds, specifically aldehydes, ketones and carboxylic acids, were strongly enriched in *B* soil gases (up to 17 % $\Sigma\text{VOCs}$  and  $0.182 \mu\text{mol/mol}$ ) with respect to those measured at both groups *A* and *C* ( $\leq 4.5$  % $\Sigma\text{VOCs}$  and up to  $0.050$  and  $0.005 \mu\text{mol/mol}$ , respectively; Fig. 2).

### 4.3 Soil fluxes

The soil  $\text{CO}_2$ ,  $\text{CH}_4$  and  $\text{H}_2\text{S}$  fluxes were measured at 81 sites in an area of about  $1,070 \text{ m}^2$  within the abandoned stone quarry. The  $\Phi\text{CO}_2$  values ranged from 13.7 to  $13,638 \text{ g m}^{-2} \text{ day}^{-1}$ , whereas lower  $\Phi\text{CH}_4$  (up to  $2.21 \text{ g m}^{-2} \text{ day}^{-1}$ ) and  $\Phi\text{H}_2\text{S}$  (up to  $74.4 \text{ g m}^{-2} \text{ day}^{-1}$ ) values were measured (Table 3).

As expected, relatively high  $\Phi\text{CO}_2$  (from 833 to  $13,638 \text{ g m}^{-2} \text{ day}^{-1}$ ),  $\Phi\text{CH}_4$  (up to  $1.54 \text{ g m}^{-2} \text{ day}^{-1}$ ) and  $\Phi\text{H}_2\text{S}$  (up to  $74.4 \text{ g m}^{-2} \text{ day}^{-1}$ ) values (Table 3) were recorded in *A* soil gas sampling sites,

1  
2  
3  
4  
5  
6  
7  
8  
9  
10  
11  
12  
13  
14  
15  
16  
17  
18  
19  
20  
21  
22  
23  
24  
25  
26  
27  
28  
29  
30  
31  
32  
33  
34  
35  
36  
37  
38  
39  
40  
41  
42  
43  
44  
45  
46  
47  
48  
49  
50  
51  
52  
53  
54  
55  
56  
57  
58  
59  
60  
61  
62  
63  
64  
65

whereas those in the *C* sites were relatively low ( $\leq 344$ ,  $\leq 0.01$  and  $\leq 0.01$  g m<sup>-2</sup> day<sup>-1</sup>, respectively; Table 3). Intermediate CO<sub>2</sub>, CH<sub>4</sub> and H<sub>2</sub>S soil fluxes (up to 3,669, 0.74 and 13.53 g m<sup>-2</sup> day<sup>-1</sup>) were measured in *B* soil sampling sites (Table 3).

In Fig. 3, the dot maps of soil CO<sub>2</sub>, CH<sub>4</sub> and H<sub>2</sub>S fluxes measured in the abandoned stone quarry are reported (Fig. 3a,c,d), together with the map of  $\Phi$ CO<sub>2</sub> values produced by the sGs method (Fig. 3b). The highest emission zone was recognized in the south-eastern portion of the study area, where the highest  $\Phi$ CO<sub>2</sub>,  $\Phi$ CH<sub>4</sub> and  $\Phi$ H<sub>2</sub>S values were measured, in agreement with previous studies (e.g. Carapezza et al., 2003, 2012). This indicates that the anomalous degassing zone is well identified in space. Such a stability supports the hypothesis of monitoring of gas emissions for hazard mitigation purposes.

#### 4.4 Measurements of air pollutants

##### 4.4.1 Gas concentrations and $\delta^{13}\text{C-CO}_2$ values in air at the fixed measuring stations

The main statistical parameters of the CO<sub>2</sub>, H<sub>2</sub>S, SO<sub>2</sub> and GEM concentrations and  $\delta^{13}\text{C-CO}_2$  values measured in F1 and F2 (Fig. 1c,e,f) in April 2016 are reported in Table 4.

At F1, CO<sub>2</sub> ranged from 874 to 1,514 mg/m<sup>3</sup> on April 5 and from 896 to 2,782 mg/m<sup>3</sup> on April 6. Throughout the time window of the survey, these values above the typical CO<sub>2</sub> concentration in air suggest that an external source of carbon dioxide concurs to the composition of air at F1 site. In those days, the H<sub>2</sub>S concentrations ranged from 53 to 982  $\mu\text{g/m}^3$  and from 41 to 568  $\mu\text{g/m}^3$ , respectively, whereas SO<sub>2</sub> air concentrations were  $\leq 33$   $\mu\text{g/m}^3$ .

At F2, the CO<sub>2</sub>, H<sub>2</sub>S and SO<sub>2</sub> concentrations, measured on April 6, were higher than those measured at F1 (up to 4,590 mg/m<sup>3</sup>, 34,407  $\mu\text{g/m}^3$  and 408  $\mu\text{g/m}^3$ , respectively). On the contrary, the highest concentrations of GEM were measured at F1 (up to 195 ng/m<sup>3</sup> on April 5), while at F2 they varied from 35 to 137 ng/m<sup>3</sup>.

1  
2  
3  
4  
5  
6  
7  
8  
9  
10  
11  
12  
13  
14  
15  
16  
17  
18  
19  
20  
21  
22  
23  
24  
25  
26  
27  
28  
29  
30  
31  
32  
33  
34  
35  
36  
37  
38  
39  
40  
41  
42  
43  
44  
45  
46  
47  
48  
49  
50  
51  
52  
53  
54  
55  
56  
57  
58  
59  
60  
61  
62  
63  
64  
65

The isotopic composition of CO<sub>2</sub> at F1 ranged from -6.49 to -1.39 ‰ vs. V-PDB and from -6.10 to 1.84 ‰ vs. V-PDB on April 5 and 6, respectively, and from -8.11 to 0.09 ‰ vs. V-PDB at F2. The carbon isotope composition indicates that carbon dioxide was enriched <sup>13</sup>C with respect to the composition of uncontaminated air ( $\delta^{13}\text{C-CO}_2 = -8\text{‰}$  vs. V-PDB). Both the less negative and positive values of  $\delta^{13}\text{C-CO}_2$  in air agree with the isotope composition of CO<sub>2</sub> emitted from F1 site, demonstrating that soil degassing governs both the concentration and the carbon isotope composition of air- CO<sub>2</sub> in the surroundings of F1 site. Furthermore, an inverse dependency of high concentration of CO<sub>2</sub> in air, positive value of  $\delta^{13}\text{C-CO}_2$  and wind speed has been observed throughout the survey.

During the air measurements in F1, the wind speed was  $\leq 1.3$  m/s on April 5, whereas on April 6 wind was basically absent. At F2, the wind speed was up to 0.9 m/s.

#### 4.4.2 Gas concentrations in air within the residential area of Cava dei Selci

The concentrations of the main air pollutants, i.e. CO<sub>2</sub>, H<sub>2</sub>S, SO<sub>2</sub>, GEM, CO and CH<sub>4</sub> were measured throughout the village of Cava dei Selci (Fig.1c,g). The main statistical parameters of these data are reported in Table 4. The concentrations of CO<sub>2</sub> ranged from 767 to 1,174 mg/m<sup>3</sup>, whereas H<sub>2</sub>S varied from 2.9 to 351  $\mu\text{g}/\text{m}^3$ . The concentrations of SO<sub>2</sub> and GEM ranged from 5.5 to 15  $\mu\text{g}/\text{m}^3$  and from 19 to 33 ng/m<sup>3</sup>, respectively. Methane and CO contents were up to 1.7 and 0.77 mg/m<sup>3</sup>, respectively. Prevailing winds (from 0 to 0.9 m/s) blew from NNE, i.e. from the main emitting areas (Fig. 1c).

Air pollutants were also measured inside one windowless private garage and one aerated basement of a house (Fig. 1g; Table 4). While the GEM concentrations in the two garages were similar (~25 ng/m<sup>3</sup>), the CO<sub>2</sub>, CO and SO<sub>2</sub> concentrations in the windowless garage were about 2 or 3 times higher than those recorded in the aerated one. Methane concentrations in the windowless garage were even 8 times higher (up to 11 mg/m<sup>3</sup>; Table 4) than those measured in the aerated basement.



1 Remarkably, H<sub>2</sub>S in the windowless garage was up to 1,358 µg/m<sup>3</sup>, i.e. more than 100 times higher  
2 than that measured in the aerated basement (up to 9.2 µg/m<sup>3</sup>).  
3  
4

## 5. Discussion

### 5.1 Origin of the endogenous gases

11 The CO<sub>2</sub>-dominated gases emitted from Cava dei Selci were characterized by δ<sup>13</sup>C-CO<sub>2</sub> values  
12 (from 0.73 to 1.08 ‰ vs. V-PDB) comparable to those reported by Minissale et al. (1997) for gas  
13 manifestations from north-central Italy. These values, significantly higher than those expected for a  
14 shallow organic derivation for CO<sub>2</sub> (typically characterized by δ<sup>13</sup>C-CO<sub>2</sub> <-20 ‰ vs. V-PDB;  
15 Degens, 1969; Rollinson, 1993; Sano and Marty, 1995), were interpreted as related to a deep high-  
16 temperature source (e.g. Giggenbach et al., 1988; Capasso et al., 1997; Chiodini and Frondini,  
17 2001; Annunziatellis et al., 2003). According to Chiodini et al. (2004), in the peri-Tyrrhenian sector  
18 of central Italy (i.e. from the Larderello geothermal field in Tuscany to the Colli Albani volcanic  
19 complex in Latium), a large portion of CO<sub>2</sub> degassing at the surface or dissolved in ground waters  
20 originates from a deep mantle-related source, which would account for a total CO<sub>2</sub> release of  
21 1.4×10<sup>11</sup> mol/y. Gases from Cava dei Selci were also characterized by a significant amount of  
22 mantle He, as indicated by the relatively high R<sub>c</sub>/R<sub>a</sub> values (1.41) that were higher than those  
23 measured in gases emitted from the other Latium volcanic districts (i.e. from 0.2 to 0.6; Hooker et  
24 al., 1985). Similar R<sub>c</sub>/R<sub>a</sub> values (from 0.44 to 1.73) were measured in fluid inclusions of  
25 phenocrysts from the Colli Albani volcanic rocks (Martelli et al., 2004; Carapezza et al., 2012).  
26 Besides the deep source, metamorphic decarbonation processes also contribute to the CO<sub>2</sub>  
27 discharged at the surface in the Colli Albani area. Giggenbach et al. (1988) ascribed the relatively  
28 high δ<sup>13</sup>C-CO<sub>2</sub> values measured in gas discharges in the Colli Albani area to the involvement of  
29 marine carbonates in the production of CO<sub>2</sub>. Carbonate assimilation in the upper crust might  
30 represent an important additional mechanism of CO<sub>2</sub> production in active volcanic zones from  
31  
32  
33  
34  
35  
36  
37  
38  
39  
40  
41  
42  
43  
44  
45  
46  
47  
48  
49  
50  
51  
52  
53  
54  
55  
56  
57  
58  
59  
60

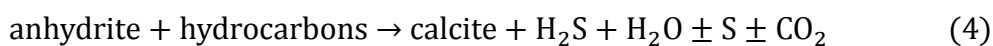
Central-Southern Italy (Iacono Marziano et al., 2007). In the  $\text{CO}_2/{}^3\text{He}$  ratios vs.  $\delta^{13}\text{C-CO}_2$  diagram (Fig. 4a), the Cava dei Selci gases plot along a mixing curve between the mantle and limestone end-members, confirming the twofold source. As shown in the Ar-N<sub>2</sub>-He ternary diagram (Fig. 4b), N<sub>2</sub> from the Cava dei Selci gases is sourced by air and a deep N<sub>2</sub>-rich source. Accordingly, the measured N<sub>2</sub>/Ar ratios (up to 134) were higher than those of both air saturated water (ASW, 38) and air (83), confirming the presence of an excess, non-atmospheric N<sub>2</sub> (N<sub>2exc</sub>). The amount of N<sub>2exc</sub> can be estimated, as follows:

$$N_{2exc} = N_2 - [(N_2/Ar)_{atm} \times Ar] \quad (3)$$

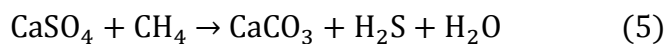
where the  $(N_2/Ar)_{atm}$  is the N<sub>2</sub>/Ar ratio in either ASW or air, assuming that Ar is entirely derived from an atmospheric component. The validity of this assumption was confirmed by the measured  ${}^{40}\text{Ar}/{}^{36}\text{Ar}$  and  ${}^{38}\text{Ar}/{}^{36}\text{Ar}$  ratios, which were comparable to those of air (i.e. 296 and 0.188, respectively; Ozima and Podosek, 2002). The N<sub>2exc</sub>/<sup>3</sup>He ratios ranged from  $4.85 \times 10^8$  to  $1.46 \times 10^9$ , i.e. higher than that expected for a pure mantle contribution (N<sub>2exc</sub>/<sup>3</sup>He ratio of  $2.3 \times 10^8$ ; Marty and Zimmermann, 1999; Hilton et al., 2002; Taran, 2011), indicating an extra-atmospheric crustal source. According to Minissale et al. (1997), the N<sub>2</sub> excess observed in several gas manifestations from north-central Italy is likely derived from organic nitrogen and ammonium-rich feldspar and micas within the Paleozoic metasedimentary basement rocks. However, the relatively low CH<sub>4</sub> contents measured in this study, in agreement with previous investigations (Annunziatellis et al., 2003; Carapezza et al., 2003; Carapezza and Tarchini, 2007), exclude the occurrence of a significant organic nitrogen source.

As far as the origin of CH<sub>4</sub> is concerned, the  $\delta^{13}\text{C-CH}_4$  values measured in gas manifestations from Cava dei Selci were higher than those expected for microbially-produced CH<sub>4</sub> ( $\leq -50$  ‰ vs. V-PDB) and thermogenic CH<sub>4</sub> (from  $-50$  to  $-30$  ‰ vs. V-PDB) (Whiticar, 1999; McCollom and Seewald, 2007). Moreover, the CH<sub>4</sub>/(C<sub>2</sub>H<sub>6</sub>+C<sub>3</sub>H<sub>8</sub>) ratio (the so-called “Bernard parameter”, after Bernard et al., 1978) varied from 214 to 231, i.e. intermediate between values characterizing gases from thermogenic (<100) and microbial sources (>1,000). Hence, the chemical and isotopic features of

CH<sub>4</sub> and light alkanes are not consistent with a classical interpretation. In Fig. 4c gas manifestations from Cava dei Selci approach the compositional field ( $\delta^{13}\text{C-CH}_4$  from -24 to -13 ‰ vs. V-PDB;  $\text{CH}_4/(\text{C}_2\text{H}_6+\text{C}_3\text{H}_8) >1,000$ ) considered by some authors (e.g. McCollom and Seewald, 2007) typical for a purely abiogenic origin. Similar values were reported by Tassi et al. (2012) for CO<sub>2</sub>-rich gas manifestations in the whole peri-Tyrrhenian part of central Italy (Tuscany and Latium) and ascribed to the addition of thermogenic gases due to secondary CH<sub>4</sub> production from CO<sub>2</sub> reduction. The occurrence of a thermogenic organic gas source at Cava dei Selci was confirmed by the presence of C<sub>4+</sub> alkanes, benzene and other aromatics. Similarly, other gas species, such as H<sub>2</sub>S and GEM, were likely produced as a result of gas reactions, re-equilibrations and mobilization processes in the hydrothermal reservoir (Minissale et al., 1997; Bagnato et al., 2009). In particular, the origin of H<sub>2</sub>S might be ascribed to thermogenic reduction of Triassic anhydrites, which are present at the base of the Mesozoic carbonate sequence (Giordano et al., 2014), as also observed in H<sub>2</sub>S-bearing gases discharging in the northern part of the Roman Magmatic Province (e.g. Sabatini and Vicano-Cimino volcanic districts; Cinti et al., 2011, 2014, 2017). In particular, the H<sub>2</sub>S production from the evaporitic formations may proceed through thermochemical sulfate reduction (TSR), a process involving hydrocarbons, according to the following reaction (Worden and Smalley, 1996):



and primarily CH<sub>4</sub>, as follows (Worden and Smalley, 1996):



## 5.2 Estimation of gas output through diffuse degassing

In order to estimate the total output of CO<sub>2</sub>, CH<sub>4</sub> and H<sub>2</sub>S from the study area, the population partitioning method proposed by Sinclair (1974) was applied. The probability plots of  $\ln\Phi_{\text{CO}_2}$ ,  $\ln\Phi_{\text{CH}_4}$  and  $\ln\Phi_{\text{H}_2\text{S}}$  are reported in Fig. 5. As suggested by Fig. 5a, most  $\ln\Phi_{\text{CO}_2}$  variations can be ascribed to a single population, with the exception of (i) some values with low  $\Phi_{\text{CO}_2}$  values ( $\leq 17$  g

1 m<sup>-2</sup> day<sup>-1</sup>), likely representing biological CO<sub>2</sub> from soil respiration and (ii) some outliers with ΦCO<sub>2</sub>  
2 ≥7,734 g m<sup>-2</sup> day<sup>-1</sup>, likely related to the occurrence of fractures causing an increase of soil  
3 permeability at a local scale. Differently from lnΦ<sub>CO<sub>2</sub></sub>, the probability plots of lnΦ<sub>CH<sub>4</sub></sub> (Fig. 5b) and  
4 lnΦ<sub>H<sub>2</sub>S</sub> (Fig. 5c) reveal the presence of two different populations (A and B). This cannot be related  
5 to the soil permeability, as this parameter should likewise affect ΦCO<sub>2</sub> producing an analogous  
6 polymodal distribution of lnΦ<sub>CO<sub>2</sub></sub>. Hence, the populations recognized in Fig. 5b,c are reflecting the  
7 occurrence of physicochemical processes affecting CH<sub>4</sub> and H<sub>2</sub>S with no influence on CO<sub>2</sub>. The  
8 total output of CO<sub>2</sub> and H<sub>2</sub>S from the study area was estimated in 2,660 and 12 kg day<sup>-1</sup>, whereas  
9 the total emission of CH<sub>4</sub> resulted in 0.42 kg day<sup>-1</sup>.  
10  
11  
12  
13  
14  
15  
16  
17  
18  
19  
20  
21  
22

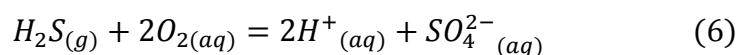
### 23 **5.3 Processes affecting gases emitted through diffuse degassing**

24  
25  
26 The soil gases emitted in the study area show anomalously high concentrations of components  
27 having non-atmospheric origin. However, the CH<sub>4</sub> and H<sub>2</sub>S concentrations in interstitial soil gases  
28 were only moderately correlated with the ΦCH<sub>4</sub> and ΦH<sub>2</sub>S values measured at the same points,  
29 whereas a better correspondence occurred between CO<sub>2</sub> and ΦCO<sub>2</sub> values (Fig. 6).  
30  
31  
32  
33  
34  
35

36 Although the CO<sub>2</sub> concentration in the soil is generally depending on biotic processes (e.g.  
37 microbial activity) and environmental factors (e.g. soil temperature and moisture content, soil  
38 permeability), the positive correlation with the ΦCO<sub>2</sub> values, clearly evident for a flux up to ≈2,500  
39 g m<sup>-2</sup> day<sup>-1</sup>, suggests that the fate of this gas in the abandoned quarry was strictly controlled by the  
40 supply of fluids from the deep reservoir. Accordingly, the CO<sub>2</sub> concentrations in interstitial soil  
41 gases are inversely correlated to those of atmospheric gases (N<sub>2</sub>, O<sub>2</sub> and Ar).  
42  
43  
44  
45  
46  
47  
48  
49

50 However, as shown in the CO<sub>2</sub>-H<sub>2</sub>S-N<sub>2</sub> ternary diagram (Fig. 7a), the CO<sub>2</sub>/H<sub>2</sub>S ratios were largely  
51 variable, ranging from 283 to 16,143, and 2-3 orders of magnitude higher than the values collected  
52 from the punctual gas emissions (from 89 to 177). It is worthwhile to mention that, during the  
53 sampling campaign in the Cava dei Selci emitting area, a shallow water table was found at around  
54 40 cm depth (locally at 20 cm depth), which is known to emerge above the ground during the rainy  
55  
56  
57  
58  
59  
60  
61  
62  
63  
64  
65

1 season forming a stagnant pool water, whose composition is strongly affected by the percolating  
2 gases (Giggenbach et al., 1988). Conversely, a certain degree of contamination of the primary deep  
3 fluids in interstitial soil gases with air-saturated water is evidenced by the N<sub>2</sub>/Ar ratio as it varies  
4 over a narrow range, from 34 to 50, i.e. similar to that of ASW. As it percolates through shallow  
5 ground waters, highly soluble H<sub>2</sub>S is oxidized, as follows:  
6  
7  
8  
9



11 Accordingly, the composition of the seasonal stagnant pool water occurring in the abandoned stone  
12 quarry was found to be characterized by a SO<sub>4</sub>-dominated composition (Giggenbach et al., 1988).  
13 Then, the two trends that can be recognized in Fig. 7a are related to (i) oxidation, and (ii) air  
14 dilution processes. A similar distribution is observed in Fig. 7b where H<sub>2</sub>S is replaced by CH<sub>4</sub>. Due  
15 to its low solubility in water, CH<sub>4</sub> is not expected to be scrubbed by the interaction of deep fluids  
16 with shallow groundwater. On the other hand, methanotrophic bacteria may catalyze the oxidation  
17 of CH<sub>4</sub> to methanol and, eventually, CO<sub>2</sub> (e.g. Rojo, 2009). Microbially-driven oxidative processes  
18 at shallow depths are generally enhanced as the diffuse degassing decreases, determining an  
19 enrichment in O-bearing organic compounds in soil gases with respect to punctual gas emissions  
20 (e.g. Tassi et al., 2015a,b and references therein). Nevertheless, A soil gases were depleted in O-  
21 bearing organic compounds relative to the gas vents and a decrease in the relative abundances of  
22 these compounds was observed in C with respect to B soil gases (Fig. 2). It has to be considered that  
23 O-bearing VOCs, such as the intermediates of CH<sub>4</sub> oxidation to CO<sub>2</sub>, are water soluble compounds  
24 due to the polarity of their molecules, thus they can be affected by the interaction with the shallow  
25 water table. Similarly, the decrease in the alkenes at decreasing CO<sub>2</sub>/N<sub>2</sub> ratios in the soil gases (Fig.  
26 2) may be related to the high reactivity of the C=C bond that makes these compounds prone to  
27 degradation processes in an aquatic environment, e.g. hydration. Selective gas dissolution may also  
28 explain the enrichment in apolar-saturated hydrocarbons (i.e. alkanes) recorded in the soil gases  
29 with respect to those occurring in the gas vents.  
30  
31  
32  
33  
34  
35  
36  
37  
38  
39  
40  
41  
42  
43  
44  
45  
46  
47  
48  
49  
50  
51  
52  
53  
54  
55  
56  
57  
58  
59  
60  
61  
62  
63  
64  
65

1 Accordingly, the chemical composition of interstitial soil gases is expected to be controlled by both  
2 (i) structural and lithological factors (e.g. brittle structures and permeability), which govern the flux  
3 of deep hydrothermal fluids, and (ii) chemical rearrangements, induced by gas-water interaction  
4 processes, microbial activity and increasingly oxidizing conditions at shallow depths. Among the  
5 endogenous gases, reduced and highly soluble species are expected to be particularly affected by  
6 secondary processes during the upward motion of fluids from the deep reservoir up to the surface,  
7 determining substantial compositional changes in gases emitted through diffuse degassing with  
8 respect to those discharged from punctual vents.  
9  
10  
11  
12  
13  
14  
15  
16  
17  
18  
19

## 20 **5.4 Impact on air quality**

### 21 **5.4.1 Fixed measuring stations**

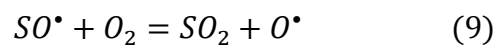
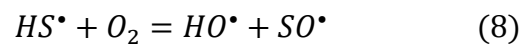
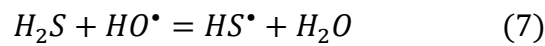
22  
23  
24  
25  
26  
27 The presence of favorable conditions to the emissions of CO<sub>2</sub>- and H<sub>2</sub>S-rich gases from the study  
28 area poses severe risks to the health of local population (e.g. Annunziatellis et al., 2003; Beaubien et  
29 al., 2003; Carapezza et al., 2003, 2010, 2012). The CO<sub>2</sub> concentrations in air measured at both the  
30 F1 and F2 measuring stations (~1,080 and 2,825 mg/m<sup>3</sup> on average, respectively) were significantly  
31 higher than the global monthly average concentration of atmospheric CO<sub>2</sub>, i.e. 733 mg/m<sup>3</sup> (Scripps  
32 CO<sub>2</sub> Program). However, the highest value (4,590 mg/m<sup>3</sup>) measured at F2 exceeded neither the 8h  
33 time weighted average (TWA) threshold of 9,000 mg/m<sup>3</sup> (NIOSH, 1996; Department of Health and  
34 Human Services - NIOSH, 2007) nor the 15 minutes short-term exposure limit (STEL) of 54,000  
35 mg/m<sup>3</sup> (NIOSH, 1996; Department of Health and Human Services - NIOSH, 2007). Nevertheless, a  
36 recent study by Martrette et al. (2017) demonstrated that prolonged exposure to relatively low CO<sub>2</sub>  
37 doses (1,260 mg/m<sup>3</sup> for 6h a day for 15 days) can cause behavioral and physiological changes in  
38 mammals, affecting general behavior, hormonal status and myosin heavy chain (MHC) profile of  
39 diaphragm and oral respiratory muscles of young female rats. Noteworthy, CO<sub>2</sub> concentrations  
40 >1,260 mg/m<sup>3</sup> were occasional at F1 and frequent at F2.  
41  
42  
43  
44  
45  
46  
47  
48  
49  
50  
51  
52  
53  
54  
55  
56  
57  
58  
59  
60  
61  
62  
63  
64  
65

1  
2  
3  
4  
5  
6  
7  
8  
9  
10  
11  
12  
13  
14  
15  
16  
17  
18  
19  
20  
21  
22  
23  
24  
25  
26  
27  
28  
29  
30  
In Fig. 8, the  $\delta^{13}\text{C-CO}_2$  values are plotted against the ratios between the concentration of  $\text{CO}_2$  in unpolluted air ( $733 \text{ mg/m}^3$ ) and the concentrations of  $\text{CO}_2$  measured at F1 and F2. The data from F2 seem to describe a mixing curve between air ( $\delta^{13}\text{C-CO}_2 = -8 \text{ ‰}$  vs. V-PDB; Scripps  $\text{CO}_2$  Program) and the endogenous  $\text{CO}_2$  source whose  $\delta^{13}\text{C-CO}_2$  value result in the range of 0.73 to 1.39 ‰ vs. V-PDB, in agreement with those measured in gases from punctual vents (Giggenbach et al., 1988; Annunziatellis et al., 2003; Carapezza and Tarchini, 2007; Carapezza et al., 2012; this study). While endogenous gas was advectively discharged at F2 through the blowing well, diffusive transport process exerted a pivotal influence on the total output of endogenous gas at F1. Accordingly, the  $\delta^{13}\text{C-CO}_2$  values measured at F1, slightly higher than those measured at F2 and expected for a simple mixing between air and endogenous gas, were likely due to isotopic fractionation processes occurring in the upper layers of soil as a consequence of gas diffusion and microbial activity (Cerling et al., 1991; Capasso et al., 2001; Camarda et al., 2007; Federico et al., 2010; Tassi et al., 2015b).

31  
32  
33  
34  
35  
36  
37  
38  
39  
40  
41  
42  
43  
44  
45  
46  
47  
48  
49  
50  
51  
52  
53  
54  
55  
56  
57  
58  
59  
60  
61  
62  
63  
64  
65  
 $\text{H}_2\text{S}$  measured in air at the fixed measuring stations ( $\geq 41 \text{ }\mu\text{g/m}^3$ ) largely exceeded the 30-min average concentration, considered as the threshold for odor annoyance in ambient air ( $7 \text{ }\mu\text{g/m}^3$ ; WHO, 2000). The average ( $213 \text{ }\mu\text{g/m}^3$ ) and maximum ( $568 \text{ }\mu\text{g/m}^3$ )  $\text{H}_2\text{S}$  air concentration measured at F1 on April 5 and 6, 2016, respectively, were significantly higher than the air quality guideline threshold ( $150 \text{ }\mu\text{g/m}^3$ ; WHO, 2000). At F2, this limit was overcome during the whole measurement period,  $\text{H}_2\text{S}$  concentrations being from 179 to  $22,238 \text{ }\mu\text{g/m}^3$ , i.e. in some cases higher than the NIOSH recommended exposure limit (REL) in workplaces ( $15,000 \text{ }\mu\text{g/m}^3$ ; Department of Health and Human Services (NIOSH), 2007). These concentrations were largely lower than those measured by Carapezza et al. (2010, 2012) from 0 to 7 a.m. (up to  $708 \text{ mg/m}^3$  at 20 cm above the ground), confirming that the risk of exposure to hazardous gas concentrations drastically increased during the night, when lack of wind and of sun irradiation favor gas accumulation at ground level (Tassi et al., 2009; Vaselli et al., 2011). At Cava dei Selci, the persistence of  $\text{H}_2\text{S}$  in air with concentrations higher than the TWA threshold in the diurnal period suggests that  $\text{H}_2\text{S}$  rather than

1  
2  
3  
4  
5  
6  
7  
8  
9  
10  
11  
12  
13  
14  
15  
16  
17  
18  
19  
20  
21  
22  
23  
24  
25  
26  
27  
28  
29  
30  
31  
32  
33  
34  
35  
36  
37  
38  
39  
40  
41  
42  
43  
44  
45  
46  
47  
48  
49  
50  
51  
52  
53  
54  
55  
56  
57  
58  
59  
60  
61  
62  
63  
64  
65

CO<sub>2</sub> represents the main threat for inhabitants in this area. The CO<sub>2</sub>/H<sub>2</sub>S ratios in the gas vents (from 89 to 177) were lower than those in air (from 1,016 to 28,139 and from 24 to 4,235 at F1 and F2, respectively), likely due to H<sub>2</sub>S oxidation in the soil (at F1) and dissolution in the well water (at F2). Further H<sub>2</sub>S consumption likely occurred in air. Whilst CO<sub>2</sub> can be considered chemically inert at ambient conditions, H<sub>2</sub>S can undergo oxidation to SO<sub>2</sub> by reacting with ozone (O<sub>3</sub>), molecular oxygen (O<sub>2</sub>) or hydroxyl radicals (HO<sup>•</sup>). The H<sub>2</sub>S oxidation involving O<sub>3</sub> and O<sub>2</sub> is slow under atmospheric conditions, thus the formation of SO<sub>2</sub> from H<sub>2</sub>S in air is likely mainly proceeding through reaction with HO<sup>•</sup> via production of HS<sup>•</sup> radical, as follows:



It is worth noting that the average SO<sub>2</sub> air concentrations exceeded the WHO guideline value of 20 µg/m<sup>3</sup> (as 24-hour average; WHO, 2006) at both F1 and F2 on 6 April, where the highest SO<sub>2</sub> air concentration approached the 10 minutes average threshold of 500 µg/m<sup>3</sup> recommended by WHO (2000, 2006), although SO<sub>2</sub> was below the detection limit in gases from the punctual vents.

These results show that secondary pollutants, i.e. those produced after the input of gases in air from a contaminant source, may have a strong impact on air quality. Sulfur dioxide is a strong-irritant gas (e.g. Petruzzi et al., 1994; Tunnicliffe et al., 2001), causing inflammation of eyes, nose and throat at 13 to 26 mg/m<sup>3</sup> and leading to respiratory failure at 79 to 105 mg/m<sup>3</sup> (WHO, 2006). Moreover, it affects trees and plants by damaging foliage and decreasing growth and contributes to acid rain, harming ecosystems and damaging materials and buildings (WHO, 2000).

#### 5.4.2 Mobile multi-instrumental station

As the prevailing winds blew from NNE, gases emitted from the abandoned stone quarry and the gas-blowing well moved towards the nearby residential area (Fig. 9). Accordingly, anomalous CO<sub>2</sub> and H<sub>2</sub>S concentrations (≥767 mg/m<sup>3</sup> and ≥2.9 µg/m<sup>3</sup>, respectively) were measured along the



1 measurement pathway, especially in the sector facing the abandoned quarry where CO<sub>2</sub> and H<sub>2</sub>S  
2 were up to 914 mg/m<sup>3</sup> and 225 µg/m<sup>3</sup>, respectively (Fig. 9a,e). The concentrations of H<sub>2</sub>S were  
3  
4 higher than the odor annoyance threshold in a large portion of the residential area and up to  
5  
6 distances >250 m from the abandoned stone quarry (Fig. 9e). Despite the common source of these  
7  
8 two gases, large variations were observed in the CO<sub>2</sub>/H<sub>2</sub>S ratios in air (from 2,592 to 203,319; Fig.  
9  
10 9b). Since the concentrations of the inert CO<sub>2</sub> in air are mainly controlled by dilution during its  
11  
12 transport from the source, the remarkable changes observed in the CO<sub>2</sub>/H<sub>2</sub>S ratios are to be ascribed  
13  
14 to either (i) chemical processes affecting and consuming H<sub>2</sub>S, i.e. chemical oxidation to SO<sub>2</sub>, or (ii)  
15  
16 different transport dynamics of the two gases in air. Whilst the CO<sub>2</sub>/H<sub>2</sub>S ratios increased as the  
17  
18 distance from the emitting area increased (Fig. 9 b), the H<sub>2</sub>S/SO<sub>2</sub> ratios decreased (Fig. 9g),  
19  
20 supporting the hypothesis of a progressive oxidation of H<sub>2</sub>S. Nevertheless, SO<sub>2</sub> concentrations  
21  
22 measured in the residential area (≤15 µg/m<sup>3</sup>; Fig. 9f) were lower than the limit (20 µg/m<sup>3</sup>) for  
23  
24 ambient air reported by WHO (2006). A relatively high H<sub>2</sub>S/SO<sub>2</sub> ratio (53; Fig. 9g) was measured  
25  
26 in correspondence with the highest CO<sub>2</sub> and H<sub>2</sub>S concentrations (1,174 mg/m<sup>3</sup> and 351 µg/m<sup>3</sup>,  
27  
28 respectively; Fig. 9a,e). Surprisingly, this measurement point was located in front of the descending  
29  
30 vehicular access to a private garage (Fig. 1g), quite far from the main emitting zone. To verify the  
31  
32 cause(s) of this anomaly, the mobile multi-instrumental station was positioned inside private  
33  
34 garages to carry out indoor measurements that revealed alarmingly high pollutants concentrations  
35  
36 (CO<sub>2</sub> concentrations up to 2,010 mg/m<sup>3</sup>, H<sub>2</sub>S and SO<sub>2</sub> concentrations exceeding the 24-h average  
37  
38 thresholds, i.e. up to 1,358 and 24.5 µg/m<sup>3</sup>, respectively). This demonstrated how the hazard related  
39  
40 to endogenous gas emission may dramatically increase under poorly ventilated conditions,  
41  
42 especially at basement and ground levels. The installation of an alarm system able to continuously  
43  
44 monitoring is highly recommended to avoid serious health problems to the inhabitants of these  
45  
46 houses.  
47  
48  
49  
50  
51  
52  
53  
54  
55  
56

57  
58 Other pollutants potentially affecting the air quality at Cava dei Selci included GEM, CO and CH<sub>4</sub>.  
59  
60 The GEM concentrations in air at F1 and F2 (up to 195 and 137 ng/m<sup>3</sup>, respectively) were  
61

1 significantly higher than the typical background concentration in unpolluted areas, i.e.  $\sim 2 \text{ ng/m}^3$   
2 (USEPA, 1997; Ebinghaus et al., 2002). Along the measuring pathway in the residential area GEM  
3  
4 ranged from 19 to  $33 \text{ ng/m}^3$ , i.e. above the mean concentrations measured in some urban  
5  
6 environments (Denis et al., 2006 and references therein). However, the GEM spatial distribution  
7  
8 was strongly different than those of  $\text{CO}_2$  and  $\text{H}_2\text{S}$  (as confirmed by the  $\text{CO}_2/\text{GEM}$  distribution map;  
9  
10 Fig. 9i), since it increased moving from NNE to SSW, the highest values being measured  $>250 \text{ m}$   
11  
12 away from the emitting area (Fig. 9h). This suggests a different transport dynamic with respect to  
13  
14  $\text{CO}_2$  and  $\text{H}_2\text{S}$ , controlled by peculiar processes regulating the behavior of the pollutant once  
15  
16 released in the air. GEM is in fact relatively stable in the atmosphere (e.g. Schroeder and Munthe,  
17  
18 1998; Sommar et al., 2001; Fitzgerald and Lamborg, 2007), having little tendency to be scavenged  
19  
20 by physical removal processes, e.g. dry deposition on vegetation (Fu et al., 2010). Moreover,  
21  
22 meteorological parameters such as temperature, humidity and wind speed and direction were proven  
23  
24 to exert a greater impact on GEM concentrations than photochemical reactions (e.g. Esbrí et al.,  
25  
26 2016), contrarily to  $\text{H}_2\text{S}$ , which is more affected by secondary (oxidation) processes in air.  
27  
28

29  
30  
31  
32  
33 The concentrations of  $\text{CO}$  and  $\text{CH}_4$  (from  $0.46$  and  $0.77 \text{ mg/m}^3$  and from  $1.3$  to  $1.7 \text{ mg/m}^3$ ,  
34  
35 respectively) were largely higher than global background concentrations ( $\leq 0.14 \text{ mg/m}^3$  and  $\sim 1.18$   
36  
37  $\text{mg/m}^3$ ; WHO, 2000). The distribution map of the  $\text{CO}_2/\text{CH}_4$  ratios (Fig. 9c) closely resembles that  
38  
39 of  $\text{CO}_2$  levels (Fig. 9a), pointing to a negligible spatial variation of the  $\text{CH}_4$  concentrations in air.  
40  
41 Moreover, the  $\text{CH}_4$  concentrations in air were comparable to those measured in other urban areas  
42  
43 ( $\sim 1.4 \text{ mg/m}^3$ ; e.g. Thi Nguyen et al., 2010), suggesting a negligible impact of the gas discharges on  
44  
45  $\text{CH}_4$  contents in ambient air in the residential area. The distribution map of the  $\text{CO}_2/\text{CO}$  ratios (Fig.  
46  
47 9d) evidences higher values in the central portion of the residential zone and a faster decrease of  $\text{CO}$   
48  
49 concentrations in air with respect to those of  $\text{CO}_2$  as the distance from the emitting source  
50  
51 increased, suggesting that  $\text{CO}$  likely undergoes oxidation processes once it is released in air.  
52  
53 Conversely, the decrease of the  $\text{CO}_2/\text{CO}$  ratios in the residential zone more distant from the emitting  
54  
55 source of endogenous gases can likely be attributed to the influence of a different contaminant  
56  
57  
58  
59  
60  
61  
62  
63  
64  
65

1 source, such as vehicular traffic. Consequently, the impact of CO due to the gas emissions is limited  
2 to the surroundings of the abandoned quarry, although the CO air levels, even inside the non-  
3 ventilated private garage, were largely lower than those measured in urban traffic environments (8-  
4 hour average CO concentrations generally lower than 20 mg/m<sup>3</sup>; WHO, 2000). Differently, CH<sub>4</sub>  
5 inside the windowless garage reached contents up to 11 mg/m<sup>3</sup>, though lighter than air, i.e. up to  
6 one order of magnitude higher than those recorded in outdoor ambient air, confirming the strong  
7 environmental effect due to the endogenous gases.  
8  
9  
10  
11  
12  
13  
14  
15  
16

## 17 **6. Conclusions**

21 Natural gas emissions and diffuse soil degassing strongly affect the air quality in the intensely  
22 urbanized area of Cava dei Selci (20 km SE of Rome) as testified by the lethal accidents that  
23 occurred in the past and caused by gas inhalation. The multi-parametric geochemical survey carried  
24 out in this area in April 2016 evidenced that CO<sub>2</sub>, mainly originated by mantle and/or magmatic  
25 degassing with a minor crustal contribution, was the main constituent of the discharged gases,  
26 followed by significant concentrations of other toxic species, such as H<sub>2</sub>S, CH<sub>4</sub> and GEM. The  
27 comparison between the chemical composition of punctual vents and soil diffuse gases revealed that  
28 secondary biogeochemical processes occurring at shallow depth (e.g. oxidation reaction, gas-water  
29 interaction and microbial activity) were able to strongly affect the reduced gas species and,  
30 consequently, they controlled the effective amounts of these species discharged into the atmosphere.  
31 Accordingly, whilst the total outputs of CO<sub>2</sub>, H<sub>2</sub>S and CH<sub>4</sub> from the study area were estimated in  
32 2,660, 12 and 0.42 kg day<sup>-1</sup>, respectively, the CO<sub>2</sub>/H<sub>2</sub>S and CO<sub>2</sub>/CH<sub>4</sub> ratios of the gases diffusively  
33 released from the soil were significantly higher than the same concentration ratios (from 89 to 177  
34 and from 1,079 to 1,456, respectively) measured in gases from the punctual emissions. Our results  
35 indicated that the effective evaluation of the potential impact of air pollutants from deep gas  
36 reservoirs requires a complete geochemical survey on both diffuse and punctual emissions.  
37  
38  
39  
40  
41  
42  
43  
44  
45  
46  
47  
48  
49  
50  
51  
52  
53  
54  
55  
56  
57  
58  
59  
60  
61  
62  
63  
64  
65

1 The air quality was estimated by a MMS approach, which produced a snapshot of the  
2 concentrations of the main deep-originated and byproduct gas compounds along a pathway passing  
3 through the urban settlement mostly exposed to the lethal gases. Hydrogen sulfide was found to be  
4 the most impacting gas, producing odor annoyance among inhabitants up to more than 250 m from  
5 the emitting area and occasionally exceeding the 24-h air quality guideline for ambient air. High  
6 concentrations of CO<sub>2</sub>, H<sub>2</sub>S and CH<sub>4</sub> were also recorded in a poorly ventilated garage likely due to  
7 gas permeation through the basement.  
8  
9

10 In the urban area of Cava dei Selci, the MMS survey coupled with a meteorological station allowed  
11 us to individuate the sites most prone to the deterioration of the air quality and provide useful  
12 information for deploying an early warning system based on gas monitoring through automated gas  
13 sensor network by the local authorities in order to avoid further lethal events and mitigate the  
14 potential hazard effects due the inhalation of toxic gases.  
15  
16

## 17 **Acknowledgments**

18 The sampling campaign at Cava dei Selci was performed in April 2016 in the framework of a field  
19 trip project ("*Studio multiparametrico sulle emissioni gassose naturali presso Cava dei Selci e*  
20 *Solfatarata di Pomezia (Colli Albani, Roma): sviluppo di un protocollo di misura per la definizione di*  
21 *traccianti geochimici atti alla valutazione dell'impatto ambientale di aree affette da degassamento*  
22 *diffuso dal suolo*") partly sponsored by So.Ge.I. (Italian Society of Geochemistry). Many thanks are  
23 due to local people for kindly providing their permission to perform air quality measurements inside  
24 their private garages and basements. We also thank Tullio Ricci and Giuseppe Etiope (National  
25 Institute of Geophysics and Volcanology INGV of Rome) for their help during the sampling  
26 session.  
27  
28

## 29 **References**

- 1  
2  
3  
4  
5  
6  
7  
8  
9  
10  
11  
12  
13  
14  
15  
16  
17  
18  
19  
20  
21  
22  
23  
24  
25  
26  
27  
28  
29  
30  
31  
32  
33  
34  
35  
36  
37  
38  
39  
40  
41  
42  
43  
44  
45  
46  
47  
48  
49  
50  
51  
52  
53  
54  
55  
56  
57  
58  
59  
60  
61  
62  
63  
64  
65
- Amato A., Chiarabba C., 1995. Recent uplift of the Alban Hills volcano (Italy), evidence for magmatic inflation? *Geophys. Res. Lett.*, 22, 1985-1988, 1995.
- Annunziatellis A., Ciotoli G., Lombardi S., Nolasco F., 2003. Short- and long-term gas hazard: the release of toxic gases in the Alban Hills volcanic area (central Italy). *J. Geochem. Explor.*, 77, 93-108, doi: 10.1016/S0375-6742(02)00272-8.
- Arthur C.L., Pawliszyn J., 1990. Solid phase microextraction with thermal desorption using fused silica optical fibers. *Anal. Chem.*, 62, 2145-2148.
- Bagnato E., Parello F., Valenza M., Caliro S., 2009. Mercury content and speciation in the Phlegrean Fields volcanic complex: Evidence from hydrothermal system and fumaroles. *J. Volcanol. Geotherm. Res.*, 187, 250-260, doi: 10.1016/j.jvolgeores.2009.09.010.
- Beaubien S.E., Ciotoli G., Lombardi S., 2003. Carbon dioxide and radon gas hazard in the Alban Hills area (central Italy). *J. Volcanol. Geotherm. Res.*, 123, 63-80, doi: 10.1016/S0377-0273(03)00028-3.
- Bernard B.B., Brooks J.M., Sackett W.M., 1978. A geochemical model for characterization of hydrocarbon gas sources in marine sediments. *Offshore Technology Conference*, Houston, USA, pp. 435-438.
- Cabassi J., Tassi F., Venturi S., Calabrese S., Capecchiacci F., D'Alessandro W., Vaselli O., 2017. A new approach for the measurement of gaseous elemental mercury (GEM) and H<sub>2</sub>S in air from anthropogenic and natural sources: Examples from Mt. Amiata (Siena, Central Italy) and Solfatara Crater (Campi Flegrei, Southern Italy). *J. Geochem. Explor.*, 175, 48-58, doi: 10.1016/j.gexplo.2016.12.017.
- Camarda M., De Gregorio S., Favara R., Gurrieri S., 2007. Evaluation of carbon isotope fractionation of soil CO<sub>2</sub> under an advective-diffusive regimen: A tool for computing the isotopic composition of unfractionated deep source. *Geochim. Cosmochim. Acta*, 71, 3016-3027, doi: 10.1016/j.gca.2007.04.002.

- 1  
2  
3  
4  
5  
6  
7  
8  
9  
10  
11  
12  
13  
14  
15  
16  
17  
18  
19  
20  
21  
22  
23  
24  
25  
26  
27  
28  
29  
30  
31  
32  
33  
34  
35  
36  
37  
38  
39  
40  
41  
42  
43  
44  
45  
46  
47  
48  
49  
50  
51  
52  
53  
54  
55  
56  
57  
58  
59  
60  
61  
62  
63  
64  
65
- Capasso G., Favara R., Inguaggiato S., 1997. Chemical features and isotopic composition of gaseous manifestations on Vulcano Island (Aeolian Islands, Italy): an interpretative model of fluid circulation. *Geochim. Cosmochim. Acta*, 61(16), 3425-3440.
- Capasso G., D'Alessandro W., Favara R., Inguaggiato S., Parello F., 2001. Kinetic isotope fractionation of CO<sub>2</sub> carbon due to diffusion processes through the soil. *Water-Rock Interaction*, 10, Swets & Zeitlinger, Lisse, 1497-1499.
- Carapezza M.L., Badalamenti B., Cavarra L., Scalzo A., 2003. Gas hazard assessment in a densely inhabited area of Colli Albani Volcano (Cava dei Selci, Roma). *J. Volcanol. Geotherm. Res.*, 123, 81-94, doi: 10.1016/S0377-0273(03)00029-5.
- Carapezza M.L., Tarchini L., 2007. Accidental gas emission from shallow pressurized aquifers at Alban Hills volcano (Rome, Italy): Geochemical evidence of magmatic degassing?. *J. Volcanol. Geotherm. Res.*, 165, 5-16, doi: 10.1016/j.jvolgeores.2007.04.008.
- Carapezza M.L., Barberi F., Tarchini L., Ranaldi M., Ricci T., 2010. Volcanic hazards of the Colli Albani. In: Funicello R., Giordano F. (eds.), *The Colli Albani Volcano*, Geological Society of London, pp. 279-297.
- Carapezza M.L., Barberi F., Ranaldi M., Ricci T., Tarchini L., Barrancos J., Fischer C., Granieri D., Lucchetti C., Melian G., Perez N., Tuccimei P., Vogel A., Weber K., 2012. Hazardous gas emissions from the flanks of the quiescent Colli Albani volcano (Rome, Italy). *Appl. Geochem.*, 27, 1767-1782, doi: 10.1016/j.apgeochem.2012.02.012.
- Cardellini C., Chiodini G., Frondini F., Granieri D., Lewicki J., Peruzzi L., 2003. Accumulation chamber measurements of methane fluxes: application to volcanic-geothermal areas and landfills. *Appl. Geochem.*, 18, 45-54.
- Cardellini C., Chiodini G., Frondini F., Avino R., Bagnato E., Caliro S., Lelli M., Rosiello A., 2017. Monitoring diffuse volcanic degassing during volcanic unrests: the case of Campi Flegrei (Italy). *Sci. Rep.* 7(1), 6757, doi: 10.1038/s41598-017-06941-2.

- 1  
2  
3  
4  
5  
6  
7  
8  
9  
10  
11  
12  
13  
14  
15  
16  
17  
18  
19  
20  
21  
22  
23  
24  
25  
26  
27  
28  
29  
30  
31  
32  
33  
34  
35  
36  
37  
38  
39  
40  
41  
42  
43  
44  
45  
46  
47  
48  
49  
50  
51  
52  
53  
54  
55  
56  
57  
58  
59  
60  
61  
62  
63  
64  
65
- Cataldi R., Mongelli F., Squarci P., Taffi L., Zito G., Calore C., 1995. Geothermal ranking of Italian territory. *Geothermics*, 24, 115-129.
- Cerling T.E., Solomon D.K., Quade J., Bowman J.R., 1991. On the isotopic composition of carbon in soil carbon dioxide. *Geochim. Cosmochim. Acta*, 55(11), 3403-3405, doi: 10.1016/0016-7037(91)90498-T.
- Chiodini G., Cioni R., Guidi M., Raco B., Marini L., 1998. Soil CO<sub>2</sub> flux measurements in volcanic and geothermal areas. *Appl. Geochem.*, 13(5), 543-552.
- Chiodini G., Frondini F., Kerrick D.M., Rogie J., Parello F., Peruzzi L., Zanzari A.R., 1999. Quantification of deep CO<sub>2</sub> fluxes from Central Italy. Examples of carbon balance for regional aquifers and of soil diffuse degassing. *Chem. Geol.*, 159, 205-222.
- Chiodini G., Frondini F., Cardellini C., Parello F., Peruzzi L., 2000. Rate of diffuse carbon dioxide Earth degassing estimated from carbon balance of regional aquifers: The case of central Apennine, Italy. *J. Geophys. Res.*, 105(B4), 8423-8434.
- Chiodini G., Frondini F., 2001. Carbon dioxide degassing from the Albani Hills volcanic region, Central Italy. *Chem. Geol.*, 177, 97-83.
- Chiodini G., Cardellini C., Amato A., Boschi E., Caliro S., Frondini F., Ventura G., 2004. Carbon dioxide Earth degassing and seismogenesis in central and southern Italy. *Geophys. Res. Lett.*, 31, L07615, doi: 10.1029/2004GL019480.
- Chiodini G., Granieri D., Avino R., Caliro S., Costa A., Werner C., 2005. Carbon dioxide diffuse degassing and estimation of heat release from volcanic and hydrothermal systems. *J. Geophys. Res.*, 110, B08204, doi:10.1029/2004JB003542.
- Chiodini G., 2008. A new web-based catalog of Earth degassing sites in Italy. *Eos*, 89(37), 341-342.
- Chiodini G., Caliro S., Cardellini C., Granieri D., Avino R., Baldini A., Donnini M., Minopoli C., 2010. Long-term variations of the Campi Flegrei, Italy, volcanic system as revealed by the monitoring of hydrothermal activity. *J. Geophys. Res.*, 115, B03205, doi:10.1029/2008JB006258.

- 1  
2  
3  
4  
5  
6  
7  
8  
9  
10  
11  
12  
13  
14  
15  
16  
17  
18  
19  
20  
21  
22  
23  
24  
25  
26  
27  
28  
29  
30  
31  
32  
33  
34  
35  
36  
37  
38  
39  
40  
41  
42  
43  
44  
45  
46  
47  
48  
49  
50  
51  
52  
53  
54  
55  
56  
57  
58  
59  
60  
61  
62  
63  
64  
65
- Chiodini G., Cardellini C., Caliro S., Chiarabba C., Frondini F., 2013. Advective heat transport associated with regional Earth degassing in central Apennine (Italy). *Earth Planet. Sci. Lett.*, 373, 65-74, doi: 10.1016/j.epsl.2013.04.009.
- Cinti D., Procesi M., Tassi F., Montegrossi G., Sciarra A., Vaselli O., Quattrocchi F., 2011. Fluid geochemistry and geothermometry in the western sector of the Sabatini Volcanic District and the Tolfa Mountains (Central Italy). *Chem. Geol.*, 284, 160-181, doi: 10.1016/j.chemgeo.2011.02.017.
- Cinti D., Tassi F., Procesi M., Bonini M., Capecchiacci F., Voltattorni N., Vaselli O., Quattrocchi F., 2014. Fluid geochemistry and geothermometry in the unexploited geothermal field of the Vicano-Cimino Volcanic District (Central Italy). *Chem. Geol.*, 371, 96-114, doi: 10.1016/j.chemgeo.2014.02.005.
- Cinti D., Tassi F., Procesi M., Brusca L., Cabassi J., Capecchiacci F., Delgado Huertas A., Galli G., Grassa F., Vaselli O., Voltattorni N., 2017. Geochemistry of hydrothermal fluids from the eastern sector of the Sabatini Volcanic District (Central Italy). *Appl. Geochem.*, 84, 187-201, doi: 10.1016/j.apgeochem.2017.06.014.
- D'Alessandro W., Brusca L., Kyriakopoulos K., Martelli M., Michas G., Papadakis G., Salerno F., 2011. Diffuse hydrothermal methane output and evidence of methanotrophic activity within the soils at Sousaki (Greece). *Geofluids*, 11, 97-107, doi: 10.1111/j.1468-8123.2010.00322.x.
- Degens E.T., 1969. Biogeochemistry of stable carbon isotopes. In: G. Eglington and M.T.J. Murphy (Eds.), *Organic Geochemistry*. Berlin-Heidelberg-New York, Springer, pp. 194-208.
- Denis M.St., Song X., Lu J.Y., Feng X., 2006. Atmospheric gaseous elemental mercury in downtown Toronto. *Atmos. Environ.*, 40(21), 4016-4024, doi: 10.1016/j.atmosenv.2005.07.078.
- Department of Health and Human Services (NIOSH), 2007. NIOSH pocket guide to chemical hazards. Cincinnati, Ohio, DHHS (NIOSH) Publication No. 2005-149, pp. 424.



- 1  
2  
3  
4  
5  
6  
7  
8  
9  
10  
11  
12  
13  
14  
15  
16  
17  
18  
19  
20  
21  
22  
23  
24  
25  
26  
27  
28  
29  
30  
31  
32  
33  
34  
35  
36  
37  
38  
39  
40  
41  
42  
43  
44  
45  
46  
47  
48  
49  
50  
51  
52  
53  
54  
55  
56  
57  
58  
59  
60  
61  
62  
63  
64  
65
- Deutsch C.V., Journel A.G., 1998. *GSLIB: Geostatistical software library and users guide*. Oxford University Press, New York, pp 1–369.
- Di Filippo M., Toro B., 1995. Gravity features. *Stratigraphy and volcano-tectonics*. In: Trigila R. (Ed.), *The Volcano of the Alban Hills*, Rome, pp. 213-219.
- Di Martino R.M.R., Capasso G., Camarda M., 2016. Spatial domain analysis of carbon dioxide from soils on Vulcano Island: Implications for CO<sub>2</sub> output evaluation, *Chem. Geol.*, 444, 59-70, doi: 10.1016/j.chemgeo.2016.09.037.
- Dubois G., 2005. An overview of radon survey in Europe. *Radioactivity Environmental Monitoring Emissions and Health Unit Institute for Environment and Sustainability JRC – European Commission*. EUR 21892 EN, EC, pp. 168.
- Ebinghaus R., Kock H.H., Coggins A.M., Spain T.G., Jennings S.G., Temme C., 2002. Long-term measurements of atmospheric mercury at Mace Head, Irish west coast, between 1995 and 2001. *Atmos. Environ.*, 36, 5267–5276, doi: 10.1016/S1352-2310(02)00691-X.
- Esbrí J.M., Martínez-Coronado A., Higuera P.L., 2016. Temporal variations in gaseous elemental mercury concentrations at a contaminated site: Main factors affecting nocturnal maxima in daily cycles. *Atmos. Environ.*, 125(A), 8-14, doi: 10.1016/j.atmosenv.2015.10.064.
- Evans W.C., White L.D., Rapp J.B., 1998. Geochemistry of some gases in hydrothermal fluids from the southern Juan de Fuca ridge. *J. Geophys. Res.*, 15, 305-313.
- Federico C., Corso P.P., Fiordilino E., Cardellini C., Chiodini G., Parello F., Pisciotta A., 2010. CO<sub>2</sub> degassing at La Solfatara volcano (Phlegrean Fields): Processes affecting  $\delta^{13}\text{C}$  and  $\delta^{18}\text{O}$  of soil CO<sub>2</sub>. *Geochim. Cosmochim. Acta*, 74, 3521-3538, doi: 10.1016/j.gca.2010.03.010.
- Fitzgerald W., Lamborg C., 2007. Geochemistry of mercury in the environment. In: Holland H, Turekian K (Eds.), *Environmental Geochemistry, Treatise on Geochemistry*. Elsevier, pp. 1–47.
- Frepoli A., Amato A., 1997. Contemporaneous extension and compression in the Northern Apennines from earthquake fault-plane solutions. *Geophys. J. Int.*, 129, 368-388.

- 1 Frondini F., Chiodini G., Caliro S., Cardellini C., Granieri D., Ventura G., 2004. Diffuse CO<sub>2</sub>  
2 degassing at Vesuvio, Italy. *Bull. Volcanol.* 66, 642-651, doi: 10.1007/s00445-004-0346-x.  
3
- 4 Fu X.W., Feng X., Dong Z.Q., Yin R.S., Wang J.X., Yang Z.R., Zhang H., 2010. Atmospheric  
5 gaseous elemental mercury (GEM) concentrations and mercury depositions at a high-  
6 altitude mountain peak in south China. *Atmos. Chem. Phys.* 10, 2425–2437.  
7
- 8 Gagliano A.L., D'Alessandro W., Tagliavia M., Parello F., Quatrini P., 2014. Methanotrophic  
9 activity and diversity of methanotrophs in volcanic geothermal soils at Pantelleria (Italy).  
10 *Biogeosciences*, 11, 5865-5875, doi: 10.5194/bg-11-5865-2014.  
11
- 12 Gellhorn E., 1936. The effect of O<sub>2</sub>-lack, variations in the CO<sub>2</sub>-content of the inspired air, and  
13 hyperpnea on visual intensity discrimination. *Am. J. Physiol.*, 115, 679-684.  
14
- 15 Giggenbach W.F., Gonfiantini R., Jangi B.L., Truesdell A.H., 1983. Isotopic and chemical  
16 composition of Parbati Valley geothermal discharges, North-West Himalaya, India.  
17 *Geothermics*, 12(2/3), 199-222.  
18
- 19 Giggenbach W.F., Minissale A.A., Scandiffio G., 1988. Isotopic and chemical assessment of  
20 geothermal potential of the Colli Albani area, Latium region, Italy. *Appl. Geochem.*, 3, 475-  
21 486.  
22
- 23 Giggenbach W.F., 1991. Chemical techniques in geothermal exploration. In: D'Amore, F. (ed.),  
24 *Application of Geochemistry in Geothermal Reservoir Development*. UNITAR, Rome, pp.  
25 119-144.  
26
- 27 Giggenbach W.F., 1996. Chemical composition of volcanic gases. In: Scarpa R, Tilling R (eds)  
28 *Monitoring and mitigation of volcano hazards*. Springer, Berlin, pp 221–256.  
29
- 30 Giordano G., De Benedetti A.A., Diana A., Diano G., Gaudioso F., Marasco F., Miceli M., Mollo  
31 S., Cas R.A.F., Funiciello R., 2006. The Colli Albani mafic caldera (Roma, Italy):  
32 Stratigraphy, structure and petrology. *J. Volcanol. Geotherm. Res.*, 155, 49-80, doi:  
33 10.1016/j.jvolgeores.2006.02.009.  
34  
35  
36  
37  
38  
39  
40  
41  
42  
43  
44  
45  
46  
47  
48  
49  
50  
51  
52  
53  
54  
55  
56  
57  
58  
59  
60  
61  
62  
63  
64  
65

- 1  
2  
3  
4  
5  
6  
7  
8  
9  
10  
11  
12  
13  
14  
15  
16  
17  
18  
19  
20  
21  
22  
23  
24  
25  
26  
27  
28  
29  
30  
31  
32  
33  
34  
35  
36  
37  
38  
39  
40  
41  
42  
43  
44  
45  
46  
47  
48  
49  
50  
51  
52  
53  
54  
55  
56  
57  
58  
59  
60  
61  
62  
63  
64  
65
- Giordano G., De Benedetti A.A., Bonamico A., Ramazzotti P., Mattei M., 2014. Incorporating surface indicators of reservoir permeability into reservoir volume calculations: Application to the Colli Albani caldera and the Central Italy Geothermal Province. *Earth Sci. Rev.*, 128, 75-92, doi: 10.1016/j.earscirev.2013.10.010.
- Glamoclija M., Garrel L., Berthon J., López-García P., 2004. Biosignatures and bacterial diversity in hydrothermal deposits of Solfatara crater, Italy. *Geomicrobiol. J.*, 21, 529-541, doi: 10.1080/01490450490888235.
- Grassa F., Capasso G., Oliveri Y., Sollami A., Carreira P Carvalho., M.R, Marques J.M., Nunes J.C, 2010. Nitrogen isotopes determination in natural gas: analytical method and first results on magmatic, hydrothermal and soil gas samples. *Isot. Environ. Health Stud.*, 46, 141-155, doi:10.1080/10256016.2010.491914.
- Henson J., Redman R., Rodriguez R., Stout R., 2005. Fungi in Yellowstone's geothermal soils and plants. *Yellowstone Science*, 13(4), 25-30.
- Hilton D.R., Fischer T.P., Marty B., 2002. Noble gases and volatile recycling at subduction zones. In: Porcelli D, Ballentine CJ, Wieler R (eds). *Noble gases in cosmochemistry and geochemistry. Rev. Mineral.* 47(1), 319–370.
- Hooker P.J., Bertrami R., Lombardi S., O’Nions R.K., Oxburgh E.R., 1985. Helium-3 anomalies and crust–mantle interaction in Italy. *Geochim. Cosmochim. Acta*, 49, 2505–2513.
- Huber R., Sacher M., Vollmann A., Huber H., Rose D., 2000. Respiration of arsenate and selenate by hyperthermophilic Archaea. *System. Appl. Microbiol.*, 23, 305-314.
- Iacono Marziano G., Gaillard F., Pichavant M., 2007. Limestone assimilation and the origin of CO<sub>2</sub> emissions at the Alban Hills (Central Italy): Constraints from experimental petrology. *J. Volcanol. Geotherm. Res.*, 166(2), 91-105, doi: 10.1016/j.jvolgeores.2007.07.001.
- Kolb C.E., Herndon S.C., McManus J.B., Shorter J.H., Zahniser M.S., Nelson D.D., Jayne J.T., Canagaratna M.R., Worsnop D.R., 2004. Mobile laboratory with rapid response instruments for real-time measurements of urban and regional trace gas and particulate distributions and

1 emission source characteristics. *Environ. Sci. Technol.*, 38, 5694–5703, doi:  
2 10.1021/es030718p.  
3

4 Langford N.J., 2005. Carbon dioxide poisoning. *Toxicol. Rev.*, 24, 229-235.  
5

6  
7 Laville P., Neri S., Continanza D., Ferrante Vero L., Bosco S., Virgili G., 2015. Cross-validation of  
8  
9 a mobile N<sub>2</sub>O flux prototype (IPNOA) using micrometeorological and chamber methods.  
10  
11 *JEPE*, 9, 375-385, doi: 10.17265/1934-8975/2015.04.007.  
12  
13

14 Mariucci M.T., Amato A., Montone P., 1999. Recent tectonic evolution and present stress in the  
15  
16 Northern Apennines (Italy). *Tectonics*, 18(1), 108-118.  
17  
18

19 Martelli M., Nuccio P.M., Stuart F.M., Burgess R., Ellam R.M., Italiano, F., 2004. Helium–  
20  
21 strontium isotope constraints on mantle evolution beneath the Roman Comagmatic Province,  
22  
23 Italy. *Earth Planet. Sci. Lett.*, 224, 295–308, doi: 10.1016/j.epsl.2004.05.025.  
24  
25

26 Martrette J.M., Egloff C., Clément C., Yasukawa K., Thornton S.N., Trabalon M., 2017. Effects of  
27  
28 prolonged exposure to CO<sub>2</sub> on behavior, hormone secretion and respiratory muscles in  
29  
30 young female rats. *Physiol. Behav.*, 177, 257-262, doi: 10.1016/j.physbeh.2017.05.007.  
31  
32

33 Marty B., Zimmermann L., 1999. Volatiles (He, C, N, Ar) in mid-ocean ridge basalts: assessment of  
34  
35 shallow-level fractionation and characterization of source composition. *Geochim.*  
36  
37 *Cosmochim. Acta*, 63, 3619–3633.  
38  
39

40  
41 Mattei M., Conticelli S., Giordano G., 2010. The Tyrrhenian margin geological setting: from the  
42  
43 Apennine orogeny to the K-rich volcanism. In: Funiciello R., Giordano G. (eds.), *The Colli*  
44  
45 *Albani Volcano. Special Publications of IAVCEI*, 3, 7-27.  
46  
47

48 McCollom T.M., Seewald J.S., 2007. Abiotic synthesis of organic compounds in deep-sea  
49  
50 hydrothermal environments. *Chem. Rev.*, 107, 382-401, doi: 10.1021/cr0503660.  
51  
52

53 Minissale A., Evans W.C., Magro G., Vaselli O., 1997. Multiple source components in gas  
54  
55 manifestations from north-central Italy. *Chem. Geol.*, 142, 175-192.  
56  
57

58 Minissale A., 2004. Origin, transport and discharge of CO<sub>2</sub> in central Italy. *Earth-Sci. Rev.*, 66, 89-  
59  
60 141, doi: 10.1016/j.earscirev.2003.09.001.  
61

- 1  
2  
3  
4  
5  
6  
7  
8  
9  
10  
11  
12  
13  
14  
15  
16  
17  
18  
19  
20  
21  
22  
23  
24  
25  
26  
27  
28  
29  
30  
31  
32  
33  
34  
35  
36  
37  
38  
39  
40  
41  
42  
43  
44  
45  
46  
47  
48  
49  
50  
51  
52  
53  
54  
55  
56  
57  
58  
59  
60  
61  
62  
63  
64  
65
- Montegrossi G., Tassi F., Vaselli O., Buccianti A., Garofalo K., 2001. Sulphur species in volcanic gases. *Anal. Chem.*, 73, 3709-3715, doi: 10.1021/ac001429b.
- NIOSH, 1996. Documentation for immediately dangerous to life or health concentrations (IDLHs) for carbon dioxide. [Available at <http://www.cdc.gov/niosh/idlh/124389.html>]
- NIST, 2005. NIST/EPA/NIH Mass Spectral Library, 2005, web site: <http://www.nist.gov/srd/nist1a.htm>.
- Norris T.B., Wraith J.M., Castenholz R.W., McDermott T.R., 2002. Soil microbial community structure across a thermal gradient following a geothermal heating event. *Appl. Environ. Microbiol.*, 68(12), 6300-6309, doi: 10.1128/AEM.68.12.6300-6309.2002.
- Olafsdottir S., Gardarsson S.M., Andradottir H.O., 2014. Natural near field sinks of hydrogen sulfide from two geothermal power plants in Iceland. *Atmos. Environ.*, 96, 236-244.
- Orlando A., Conticelli S., Manetti P., Vaggelli G., 1994. The basement of northern Vulsinian volcanic District as inferred from the study of crustal xenoliths from the Torre Alfina lavas, Viterbo, central Italy. *Mem. Soc. Geol. It.*, 48, 681- 688.
- Ozima M., Podosek F.A., 2002. Noble gas geochemistry, 2nd ed. Cambridge University Press, Cambridge, 286 pp.
- Paonita A., Caracausi A., Iacono-Marziano G., Martelli M., Rizzo A., 2012. Geochemical evidence for mixing between fluids exsolved at different depths in the magmatic system of Mt Etna (Italy). *Geochim. Cosmochim. Acta*, 84, 380-394, doi: 10.1016/j.gca.2012.01.028.
- Peccerillo A., 1999. Multiple mantle metasomatism in central-southern Italy: geochemical effects, timing and geodynamic implications. *Geology*, 27, 315-318.
- Peccerillo A., 2005. Plio-Quaternary volcanism in Italy. *Petrology, Geochemistry, Geodynamics*. Springer, Heidelberg, pp. 365.
- Peralta O., Castro T., Durón M., Salcido A., Celada-Murillo A.T., Navarro-González R., Márquez C., García J., de la Rosa J., Torres R., Villegas-Martínez R., Carreón-Sierra S., Imaz M., Martínez-Arroyo A., Saavedra I., de la Luz E.M., Torres-Jaramillo A., 2013. H<sub>2</sub>S emissions

1 from Cerro Prieto geothermal power plant, Mexico, and air pollutants measurements in the  
2 area. *Geothermics*, 46, 55–65.  
3

4 Petruzzi S., Musi B., Bignami G., 1994. Acute and chronic sulphur dioxide (SO<sub>2</sub>) exposure: an  
5 overview of its effects on humans and laboratory animals. *Ann. Ist. Super. Sanità*, 30(2),  
6 151-156.  
7

8 Pizzino L., Galli G., Mancini C., Quattrocchi F., Scarlato P., 2002. Natural Gas Hazard (CO<sub>2</sub>,  
9 <sup>222</sup>Rn) within a Quiescent Volcanic Region and Its Relations with Tectonics: The Case of  
10 the *Ciampino-Marino* Area, Alban Hills Volcano, Italy. *Nat. Hazards*, 27, 257-287.  
11

12 Rogie J.D., Kerrick D.M., Chiodini G., Frondini F., 2000. Flux measurements of nonvolcanic CO<sub>2</sub>  
13 emission from some vents in central Italy. *J. Geophys. Res.*, 105(B4), 8435-8445.  
14

15 Rojo F., 2009. Degradation of alkanes by bacteria. *Environ. Microbiol.*, 11(10), 2477-2490, doi:  
16 10.1111/j.1462-2920.2009.01948.x.  
17

18 Rollinson H., 1993. Using geochemical data. Longman, London, UK, p. 352.  
19

20 Sano Y., Marty B., 1995. Origin of carbon in fumarolic gas from island arcs. *Chem. Geol. (Isotope*  
21 *Geoscience Section)*, 119, 265-274.  
22

23 Schroeder W.H., Munthe J., 1998. Atmospheric mercury—an overview. *Atmos. Environ.* 32, 809–  
24 822.  
25

26 Scripps CO<sub>2</sub> Program, Scripps Institution of Oceanography UC San Diego,  
27 <http://scrippsco2.ucsd.edu>.  
28

29 Scrocca D., Doglioni C., Innocenti F., 2003. Constraints for an interpretation of the Italian  
30 geodynamics: a review. *Mem. Descr. Carta Geologica d'It.*, 62, 15-46.  
31

32 Sechzer P.H., Egbert L.D., Linde H.W., Cooper D.Y., Dripps R.D., Price H.L., 1960. Effect of CO<sub>2</sub>  
33 inhalation on arterial pressure, ECG and plasma catecholamines and 17-OH corticosteroids  
34 in normal man. *J. Appl. Physiol.*, 15, 454-458.  
35

36 Sholupov S.E., Ganeyev A.A., 1995. Zeeman atomic absorption spectrometry using high frequency  
37 modulated light polarization. *Spectrochim. Acta B At. Spectrosc.* 50, 1227–1236.  
38

- 1 Sholupov S., Pogarev S., Ryzhov V., Mashyanov N., Stroganov A., 2004. Zeeman atomic  
2 absorption spectrometer RA-915+ for direct determination of mercury in air and complex  
3 matrix samples. *Fuel Process. Technol.* 85, 473–485.  
4  
5  
6  
7 Sinclair A.J., 1974. Selection of threshold values in geochemical data using probability graphs. *J.*  
8  
9 *Geochem. Explor.* 3, 129-149.  
10  
11 Sommar J., Gårdfeldt K., Strömberg D., Feng X., 2001. A kinetic study of the gas-phase reaction  
12 between the hydroxyl radical and atomic mercury. *Atmos. Environ.* 35, 3049–3054.  
13  
14  
15  
16 Taran Y., 2011. N<sub>2</sub>, Ar, and He as a tool for discriminating sources of volcanic fluids with  
17 application to Vulcano, Italy. *Bull. Volcanol.*, 73, 395-408, doi: 10.1007/s00445-011-0448-  
18  
19 1.  
20  
21  
22  
23  
24 Tassi F., Vaselli O., Cuccoli F., Buccianti A., Nisi B., Lognoli E., Montegrossi G., 2009. A  
25 geochemical multi-methodological approach in hazard assessment of CO<sub>2</sub>-rich gas  
26 emissions at Mt. Amiata volcano (Tuscany, Central Italy). *Water Air & Soil Pollution:*  
27  
28 *Focus*, 9(1-2), 117-127, doi: 10.1007/s11267-008-9198-2.  
29  
30  
31  
32  
33  
34 Tassi F., Fiebig J., Vaselli O., Nocentini M., 2012. Origins of methane discharging from volcanic-  
35 hydrothermal emissions in Italy. *Chem. Geol.*, 310-311, 36-48, doi:  
36  
37 10.1016/j.chemgeo.2012.03.018.  
38  
39  
40  
41 Tassi F., Nisi B., Cardellini C., Capecchiacci F., Donnini M., Vaselli O., Avino R., Chiodini G.,  
42  
43 2013. Diffuse soil emission of hydrothermal gases (CO<sub>2</sub>, CH<sub>4</sub>, C<sub>6</sub>H<sub>6</sub>) at Solfatara crater  
44 (Campi Flegrei, southern Italy). *Appl. Geochem.*, 35, 142-153, doi:  
45  
46 10.1016/j.apgeochem.2013.03.020.  
47  
48  
49  
50  
51 Tassi F., Venturi S., Cabassi J., Capecchiacci F., Nisi B., Vaselli O., 2015a. Volatile organic  
52 compounds (VOCs) in soil gases from Solfatara crater (Campi Flegrei, southern Italy):  
53  
54 Geogenic source(s) vs. biogeochemical processes. *Appl. Geochem.*, 56, 37-49, doi:  
55  
56 10.1016/j.apgeochem.2015.02.005.  
57  
58  
59  
60  
61  
62  
63  
64  
65

- 1  
2 Tassi F., Venturi S., Cabassi J., Vaselli O., Gelli I., Cinti D., Capecchiacci F., 2015b.  
3 Biodegradation of CO<sub>2</sub>, CH<sub>4</sub> and volatile organic compounds (VOCs) in soil gas from the  
4 Vicano-Cimino hydrothermal system (central Italy). *Org. Geochem.*, 86, 81-93, doi:  
5 10.1016/j.orggeochem.2015.06.004.  
6  
7  
8  
9 Thermo Fisher Scientific Inc, 2012. Thermo Scientific Model 450i Hydrogen Sulfide & Sulfur  
10 Dioxide Analyzer Manual. Link.  
11 [https://www.thermoscientific.com/content/dam/tfs/ATG/EPD/EPD%20Documents/Product](https://www.thermoscientific.com/content/dam/tfs/ATG/EPD/EPD%20Documents/Product%20Manuals%20&%20Specifications/Air%20Quality%20Instruments%20and%20Systems/Ambient%20Gas/D19731~.pdf)  
12 [%20Manuals%20&%20Specifications/Air%20Quality%20Instruments%20and%20Systems/](https://www.thermoscientific.com/content/dam/tfs/ATG/EPD/EPD%20Documents/Product%20Manuals%20&%20Specifications/Air%20Quality%20Instruments%20and%20Systems/Ambient%20Gas/D19731~.pdf)  
13 [Ambient%20Gas/D19731~.pdf](https://www.thermoscientific.com/content/dam/tfs/ATG/EPD/EPD%20Documents/Product%20Manuals%20&%20Specifications/Air%20Quality%20Instruments%20and%20Systems/Ambient%20Gas/D19731~.pdf).  
14  
15  
16  
17  
18  
19  
20  
21 Thi Nguyen H., Kim K.H., Ma C.J., Cho S.J., Ryeul Sohn J., 2010. A dramatic shift in CO and CH<sub>4</sub>  
22 levels at urban locations in Korea after the implementation of the Natural Gas Vehicle  
23 Supply (NGVS) program. *Environ. Res.*, 110(4), 396-409, doi:  
24 10.1016/j.envres.2010.03.002.  
25  
26  
27  
28  
29  
30  
31 Trigila R., Agosta E., Currado C., De Benedetti A.A., Freda C., Gaeta M., Palladino D.M., Rosa C.,  
32 1995. Petrology. In: Trigila R. (ed.), *The Volcano of the Alban Hills*. Tipografia S.G.S.,  
33 Roma, 95– 165.  
34  
35  
36  
37  
38  
39 Tunnicliffe W.S., Hilton M.F., Harrison R.M., Ayres J.G., 2001. The effect of sulphur dioxide  
40 exposure on indices of heart rate variability in normal and asthmatic adults. *Eur. Respir. J.*  
41 17 (4), 604–608.  
42  
43  
44  
45  
46 USEPA, 1997. Mercury study report to congress. EPA-452/R-97-005. Fate and Transport of  
47 Mercury in the Environment III. U.S. Environmental Protection Agency.  
48  
49  
50  
51 Vaselli O., Tassi F., Montegrossi G., Capaccioni B., Giannini L., 2006. Sampling and analysis of  
52 volcanic gases. *Acta Vulcanol.*, 18(1-2), 65-76.  
53  
54  
55  
56 Vaselli O., Nisi B., Tassi F., Rappuoli D., Pancioli V., Ucciero S., Giannini L., 2011. CO<sub>2</sub> hazard vs  
57  
58  
59  
60  
61  
62  
63  
64  
65



1 Whiticar M.J., 1999. Carbon and hydrogen isotope systematics of bacterial formation and oxidation  
2 of methane. Chem. Geol., 161, 291-314.  
3

4 WHO, 2000. Air quality guidelines for Europe, second ed. WHO Regional Publications. European  
5 Series, No. 91.  
6  
7

8 WHO, 2006. Air quality guidelines for particulate matter, ozone, nitrogen dioxide and sulfur  
9 dioxide. Global update 2005. Summary of risk assessment. World Health Organization  
10  
11  
12  
13  
14  
15  
16  
17  
18  
19  
20  
21  
22  
23  
24  
25  
26  
27  
28  
29  
30  
31  
32  
33  
34  
35  
36  
37  
38  
39  
40  
41  
42  
43  
44  
45  
46  
47  
48  
49  
50  
51  
52  
53  
54  
55  
56  
57  
58  
59  
60  
61  
62  
63  
64  
65

66 Worden R.H., Smalley P.C., 1996. H<sub>2</sub>S-producing reactions in deep carbonate gas reservoirs: Khuff  
67 Formation, Abu Dhabi. Chem. Geol., 133, 157-171.  
68  
69  
70  
71  
72  
73  
74  
75  
76  
77  
78  
79  
80  
81  
82  
83  
84  
85  
86  
87  
88  
89  
90  
91  
92  
93  
94  
95  
96  
97  
98  
99  
100

## Table captions

**Table 1** Chemical and isotope compositions of gases emitted from punctual gas emissions at Cava dei Selci. The concentrations of inorganic gas species and methane are expressed in mmol/mol, whilst the contents of organic compounds are reported in  $\mu\text{mol/mol}$ . The  $\delta^{13}\text{C}$  values of  $\text{CO}_2$  and  $\text{CH}_4$  are expressed in delta ( $\delta$ ) per mil (‰) against Vienna Pee Dee Belemnite (V-PDB).

**Table 2** Chemical composition of main gas species ( $\text{CO}_2$ ,  $\text{H}_2\text{S}$ ,  $\text{N}_2$ ,  $\text{O}_2$ , Ar,  $\text{CH}_4$ , in mmol/mol) and VOCs (in  $\mu\text{mol/mol}$ ) in interstitial soil gas samples from Cava dei Selci.

**Table 3** Soil  $\text{CO}_2$ ,  $\text{CH}_4$  and  $\text{H}_2\text{S}$  fluxes (expressed in  $\text{g m}^{-2} \text{day}^{-1}$ ) measured in the abandoned stone quarry of Cava dei Selci.

**Table 4** Summary statistics (minimum, maximum, average and standard deviation) of atmospheric concentrations of  $\text{CO}_2$ ,  $\text{H}_2\text{S}$ ,  $\text{SO}_2$ , GEM, CO and  $\text{CH}_4$  and  $\delta^{13}\text{C}\text{-CO}_2$  values recorded by the fixed measuring stations (F1 and F2), in the residential area of Cava dei Selci and inside two private garages.

## Figure captions

**Fig. 1** (a) Satellite image of Latium (Italy) with the location of Colli Albani and Rome. (b) Satellite image of the Colli Albani area, from Ciampino airport to Lake Albano. The location of Cava dei Selci is reported. (c) Satellite image of Cava dei Selci. The emitting areas from the abandoned stone quarry and the gas-blowing well are counteracted with a dashed yellow line, together with the residential area where real-time continuous measurements of air quality were performed. (d) Photograph of the abandoned stone quarry in front of the houses of Cava dei Selci. (e) Photograph of the gas-blowing well and the fixed measuring station at F2 for air quality measurements. (f) Location of the sampling sites where the punctual gas emissions (G1 and G2; black circles) and interstitial soil gases (*A* soil gases: orange circles; *B* soil gases: green circles; *C* soil gases: blue

1 circles) were collected and position of the fixed measuring station for air quality measurements (F1;  
2 white square) in the abandoned stone quarry. (g) Photograph of the mobile prototype for real-time  
3 continuous measurements of air quality together with location and photographs of, clockwise from  
4 top right, the windowless garage, the aerated garage and the descending vehicular access to a  
5 private garage.  
6  
7  
8  
9  
10

11  
12 **Fig. 2** Box plots of relative abundances (expressed as % $\Sigma$ VOCs) of alkanes, aromatics, alkenes,  
13 cyclics, S-bearing compounds, aldehydes+ketones+carboxylic acids, and other VOCs in A (orange  
14 boxes), B (green boxes) and C (blue boxes) soil gases from Cava dei Selci.  
15  
16  
17  
18  
19  
20

21 **Fig. 3** Dot maps of soil (a) CO<sub>2</sub>, (c) H<sub>2</sub>S and (d) CH<sub>4</sub> fluxes measured in the abandoned stone  
22 quarry of Cava dei Selci. (b) The map of  $\Phi$ CO<sub>2</sub> values produced by sGs method is also reported.  
23  
24  
25  
26

27 **Fig. 4** (a) CO<sub>2</sub>/<sup>3</sup>He vs.  $\delta^{13}$ C-CO<sub>2</sub> binary diagram (after Sano and Marty, 1995) for punctual gas  
28 emissions from Cava dei Selci (black circles = data from this study; white circles = data from  
29 Carapezza and Tarchini, 2007; Carapezza et al., 2012). Mid-ocean ridge basalt (MORB), limestone  
30 and sediment fields are also indicated. (b) Ar-N<sub>2</sub>-He ternary diagram (after Giggenbach et al., 1983;  
31 Giggenbach, 1991, 1996) for gases discharged from Cava dei Selci (black circles = data from this  
32 study; white circles = data from Giggenbach et al., 1988; Chiodini and Frondini, 2001; Carapezza et  
33 al., 2012). Andesitic, mantle and crustal end-members are also reported, together with those of air  
34 and air saturated water (ASW). (c) CH<sub>4</sub>/(C<sub>2</sub>H<sub>6</sub>+C<sub>3</sub>H<sub>8</sub>) vs.  $\delta^{13}$ C-CH<sub>4</sub> binary diagram for punctual gas  
35 emissions from Cava dei Selci (after Bernard et al., 1978; Whiticar, 1999). Existence fields of  
36 biogenic origin (microbial and thermogenic) and unsedimented mid-oceanic ridges, sediment-  
37 covered ridges and igneous rocks are reported (McCollom and Seewald, 2007, and references  
38 therein) for comparison.  
39  
40  
41  
42  
43  
44  
45  
46  
47  
48  
49  
50  
51  
52  
53  
54  
55  
56

57 **Fig. 5** Probability plots of (a)  $\ln\Phi_{\text{CO}_2}$ , (b)  $\ln\Phi_{\text{CH}_4}$  and (c)  $\ln\Phi_{\text{H}_2\text{S}}$ .  
58  
59  
60  
61  
62  
63  
64  
65

1  
2 **Fig. 6** (a)  $\text{CO}_2$  vs.  $\Phi\text{CO}_2$ , (b)  $\text{CH}_4$  vs.  $\Phi\text{CH}_4$  and (c)  $\text{H}_2\text{S}$  vs.  $\Phi\text{H}_2\text{S}$  binary diagrams (*A* soil gases:  
3 orange circles; *B* soil gases: green circles; *C* soil gases: blue circles).

4  
5 **Fig. 7** (a)  $\text{CO}_2$ - $\text{H}_2\text{S}$ - $\text{N}_2$  and (b)  $\text{CO}_2$ - $\text{CH}_4$ - $\text{N}_2$  ternary diagrams for interstitial soil gases (*A* soil gases:  
6 orange circles; *B* soil gases: green circles; *C* soil gases: blue circles) and punctual gas emissions  
7 (black circles).  
8  
9

10  
11 **Fig. 8**  $\delta^{13}\text{C}$ - $\text{CO}_2$  vs.  $733/\text{CO}_2$  binary diagram of air measurements in F1 on April 5 (violet squares)  
12 and 6 (red squares) and in F2 (yellow squares). Air and endogenous gas (grey fields) are plotted for  
13 comparison.  
14  
15  
16  
17  
18  
19  
20  
21

22 **Fig. 9** Dot maps of air concentrations of (a)  $\text{CO}_2$ , (e)  $\text{H}_2\text{S}$ , (f)  $\text{SO}_2$ , (h) GEM and concentration  
23 ratios of (b)  $\text{CO}_2/\text{H}_2\text{S}$ , (c)  $\text{CO}_2/\text{CH}_4$ , (d)  $\text{CO}_2/\text{CO}$ , (g)  $\text{H}_2\text{S}/\text{SO}_2$  and (i)  $\text{CO}_2/\text{GEM}$  measured in the  
24 residential area in Cava dei Selci. The yellow dashed ellipse identifies the location of the abandoned  
25 quarry. (l) Wind direction and speed.  
26  
27  
28  
29  
30  
31  
32  
33  
34  
35  
36  
37  
38  
39  
40  
41  
42  
43  
44  
45  
46  
47  
48  
49  
50  
51  
52  
53  
54  
55  
56  
57  
58  
59  
60  
61  
62  
63  
64  
65

Table 1

	<b>G1</b>	<b>G2</b>	<b>G3</b>
<b>CO<sub>2</sub></b>	985	982	990
<b>H<sub>2</sub>S</b>	9.2	11	5.6
<b>N<sub>2</sub></b>	4.3	5.6	3.2
<b>O<sub>2</sub></b>	0.13	0.087	0.095
<b>Ar</b>	0.032	0.051	0.026
<b>Ne</b>	0.000078		0.000013
<b>He</b>	0.0011		0.0011
<b>H<sub>2</sub></b>	0.036	0.056	0.015
<b>CO</b>	0.0033	0.0009	0.0013
<b>CH<sub>4</sub></b>	0.82	0.91	0.68
<b>δ<sup>13</sup>C-CO<sub>2</sub></b>	1.08	0.9	0.73
<b>δ<sup>13</sup>C-CH<sub>4</sub></b>	-29	-30	-32
<b>R/R<sub>a</sub></b>	1.40		1.41
<b>R<sub>c</sub>/R<sub>a</sub></b>	1.41		1.41
<b><sup>40</sup>Ar/<sup>36</sup>Ar</b>	293		299
<b><sup>38</sup>Ar/<sup>36</sup>Ar</b>	0.19		0.19
<b>C<sub>2</sub>H<sub>6</sub></b>	3.3	3.6	2.5
<b>C<sub>3</sub>H<sub>8</sub></b>	0.51	0.66	0.44
<b>iC<sub>4</sub>H<sub>10</sub></b>	0.16	0.15	0.21
<b>nC<sub>4</sub>H<sub>10</sub></b>	0.22	0.18	0.25
<b>C<sub>5+</sub> alkanes</b>	0.71	0.69	0.56
<b>C<sub>6</sub>H<sub>6</sub></b>	0.61	0.64	0.47
<b>branched aromatics</b>	0.64	0.78	0.61
<b>kenotes</b>	0.15	0.60	0.28
<b>aldehydes</b>	0.15	0.13	0.11
<b>esters+acids</b>	2.4	2.1	1.8
<b>S-substituted</b>	1.7	2.5	3.9
<b>others</b>	0.24	0.39	0.11

Table 2

ID	Depth	Type	CO <sub>2</sub>	H <sub>2</sub> S	N <sub>2</sub>	O <sub>2</sub>	Ar	CH <sub>4</sub>	C <sub>2</sub> H <sub>6</sub>	C <sub>3</sub> H <sub>8</sub>
1	20	C	272		498	218	12	0.023	0.085	0.011
2	10	A	903	1.3	89	4.4	2.2	0.058	0.24	0.075
3	10	B	886	2.1	101	8.1	2.3	0.067	0.31	0.087
4	20	A	934	3.3	59	1.6	1.4	0.075	0.44	0.11
5	20	A	928	3.2	66	1.2	1.6	0.044	0.21	0.061
6	20	A	907	2.6	81	6.8	1.9	0.075	0.39	0.061
7	20	B	843	0.13	131	22	3.4	0.019	0.077	0.012
8	10	C	4.9		665	315	15	0.015	0.065	0.011
9	20	A	917	2.4	77	1.4	1.8	0.055	0.23	0.075
10	20	A	913	1.9	81	1.5	1.9	0.13	0.61	0.15
11	20	B	886	1.1	104	5.4	2.5	0.12	0.52	0.11
12	20	C	19		671	295	15	0.026	0.095	0.014
13	20	A	928	0.88	66	3.6	1.6	0.036	0.18	0.032
14	20	A	944	1.9	51	1.5	1.4	0.11	0.56	0.096
15	20	A	948	0.64	48	2.1	1.4	0.022	0.091	0.015
16	20	A	920	0.14	76	2.3	1.8	0.025	0.11	0.023
17	20	C	299		484	205	12	0.011	0.056	0.0095
18	20	A	962	0.39	36	0.51	0.85	0.098	0.47	0.086
19	20	C	302		551	136	11	0.021	0.074	0.005
20	20	B	508		395	87	9.6	0.018	0.066	0.004
21	20	B	498		388	104	9.9	0.015	0.052	0.003
22	20	B	831	0.056	131	35	3.3	0.041	0.14	0.045
23	20	B	846	0.22	125	26	3.1	0.034	0.13	0.042
24	20	B	759	0.12	187	49	4.7	0.023	0.088	0.012
25	20	B	640	0.13	284	69	6.7	0.021	0.087	0.01
26	20	B	882	0.056	103	12	2.5	0.026	0.096	0.011
27	20	B	896	0.12	94	7.8	2.3	0.014	0.057	0.008
28	20	B	689	0.069	256	48	6.4	0.011	0.036	0.005
29	20	A	904	0.056	87	6.6	2.1	0.046	0.21	0.035
30	20	B	876	0.46	115	5.1	2.8	0.054	0.28	0.049
31	20	A	900	0.29	86	12	1.9	0.024	0.12	0.025
32	20	B	745	0.095	185	66	4.2	0.019	0.094	0.011
33	20	B	599	0.087	381	11	9.2	0.023	0.11	0.021
34	20	B	744	0.11	215	36	4.7	0.021	0.085	0.015
35	20	B	742	0.12	202	51	4.5	0.022	0.091	0.017

**Table 3**

<b>ID</b>	<b><math>\Phi\text{CO}_2</math></b>	<b><math>\Phi\text{CH}_4</math></b>	<b><math>\Phi\text{H}_2\text{S}</math></b>
1	122	0.01	
2	5125	0.74	14.19
3	3669	0.74	13.53
4	13638	1.54	20.45
5	12640	1.50	74.40
6	7734	0.94	44.64
7	1030	0.04	
8	14		0.01
9	5191	0.94	14.73
10	4373	0.79	12.28
11	1319	0.15	5.37
12	16		
13	833	0.10	4.56
14	8134	1.14	14.44
15	1257	0.19	1.91
16	895	0.13	
17	344		
18	956	0.13	3.05
19	83		
20	114		
21	159		
22	2022	0.29	
23	1939	0.32	0.22
24	1223	0.14	0.04
25	842	0.10	0.02
26	1425	0.11	
27	2109	0.09	0.02
28	541		
29	2011	0.33	
30	2012	0.25	0.59
31	1063	0.04	0.03
32	661		
33	194		
34	461		
35	550		0.01
36	113		
37	1122	0.06	
38	3270	0.21	
39	212	0.03	
40	2865	0.12	0.07
41	889	0.10	
42	17	0.00	
43	1100	0.11	
44	144	0.01	
45	237		0.01
46	484	0.01	
47	339	0.00	0.00
48	338	0.02	
49	191		

Table 4

	Date	Time Interval	CO <sub>2</sub> (mg/m <sup>3</sup> )				H <sub>2</sub> S (	
			min	max	average	st.dev.	min	max
<b>F1</b>	April 5, 2016	14:51-18:01	874	1,514	1,086	133	53	982
<b>F1</b>	April 6, 2016	10:52-12:10	896	2,782	1078	235	41	568
<b>F2</b>	April 6, 2016	16:36-17:32	809	4,590	2,825	1211	179	34,407
<b>Residential area</b>	April 7, 2016	09:34-11:23	767	1,174	807	64	2.9	351
<b>Aerated garage</b>	April 7, 2016	09:44-09:49	792	916	864	46	7.6	9.2
<b>Windowless garage</b>	April 7, 2016	10:11-10:15	1,776	2,010	1,861	80	1,095	1,358



Figure 1  
[Click here to download high resolution image](#)

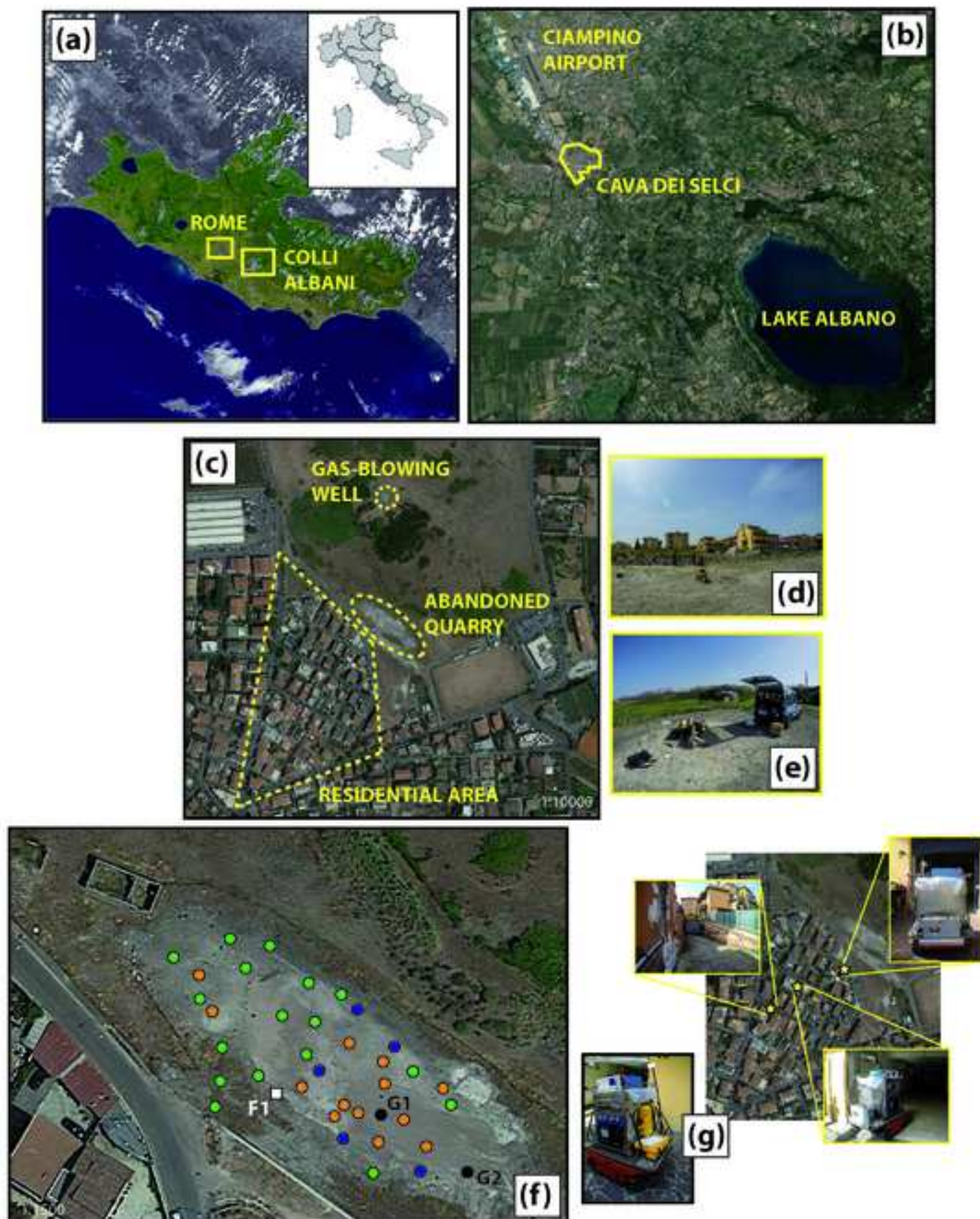


Figure 2

[Click here to download high resolution image](#)

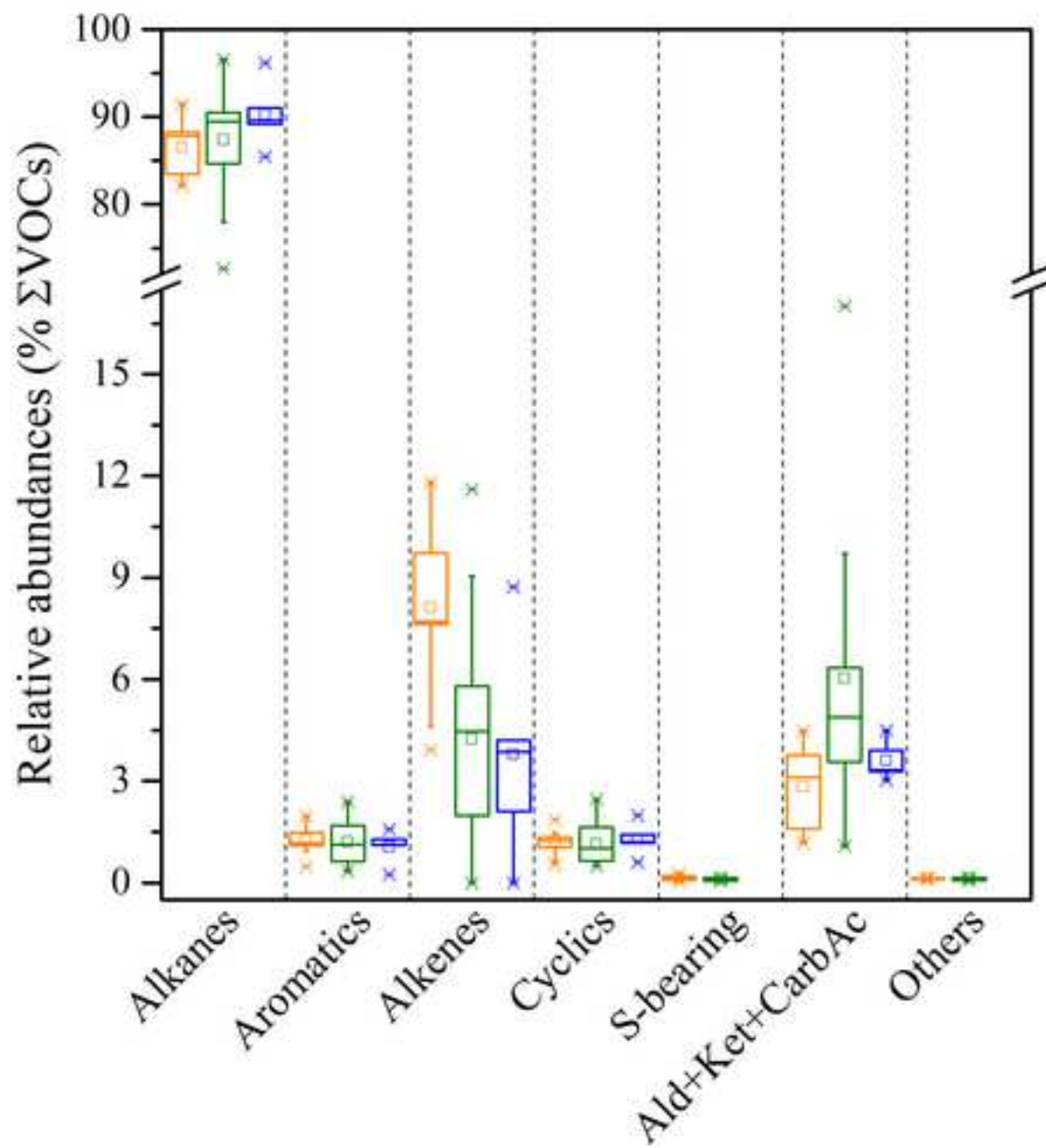


Figure 3  
[Click here to download high resolution image](#)

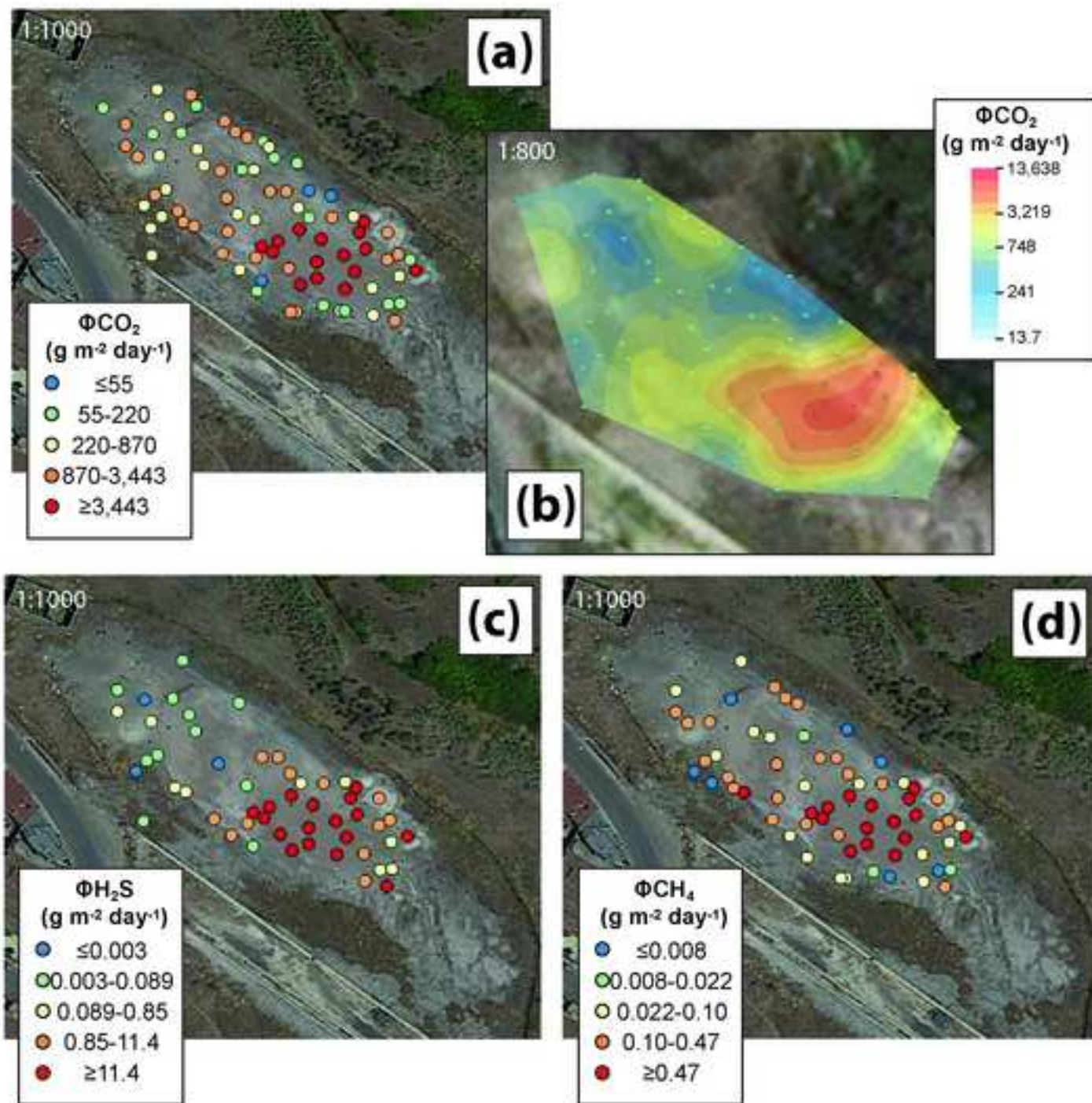


Figure 4  
[Click here to download high resolution image](#)

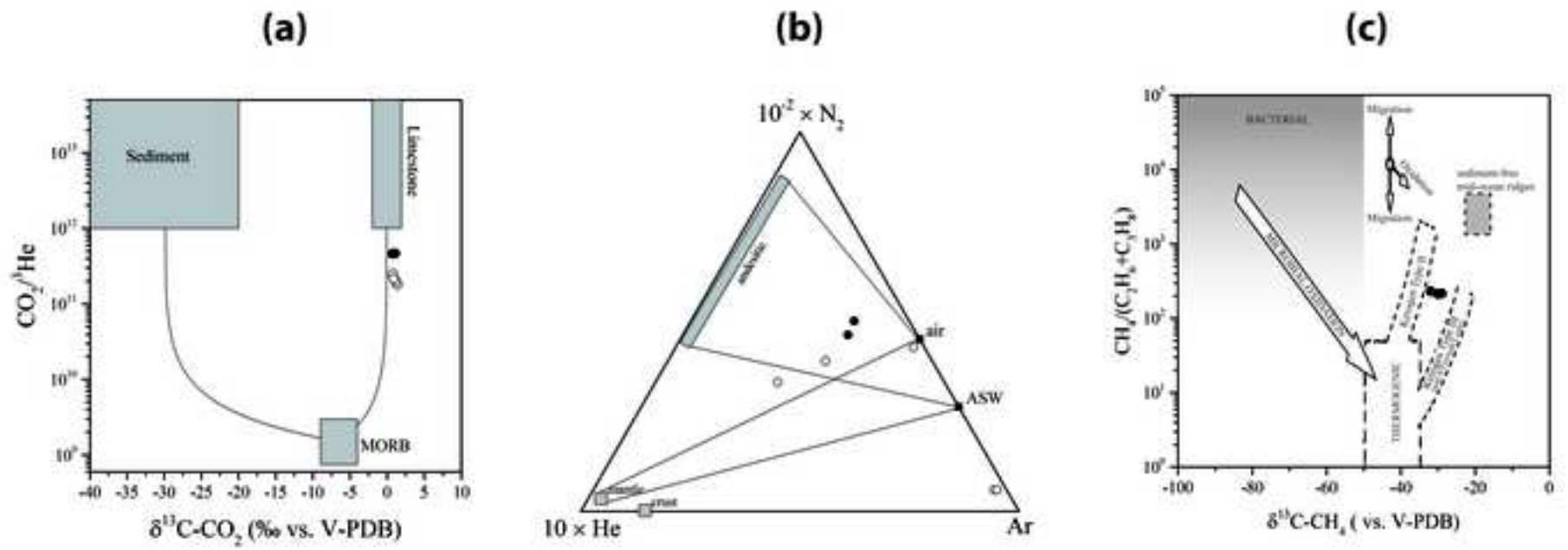


Figure 5

[Click here to download high resolution image](#)

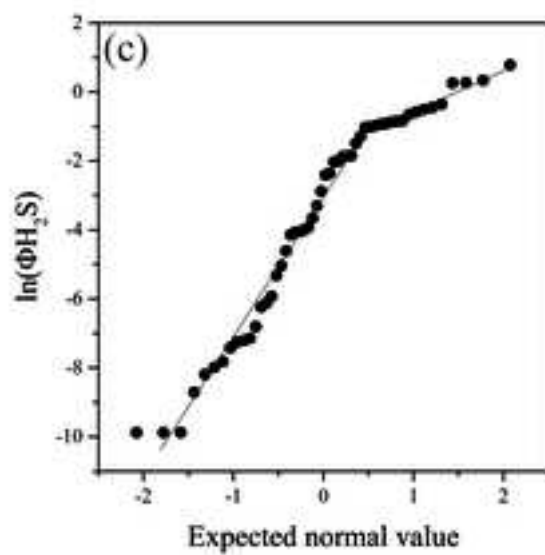
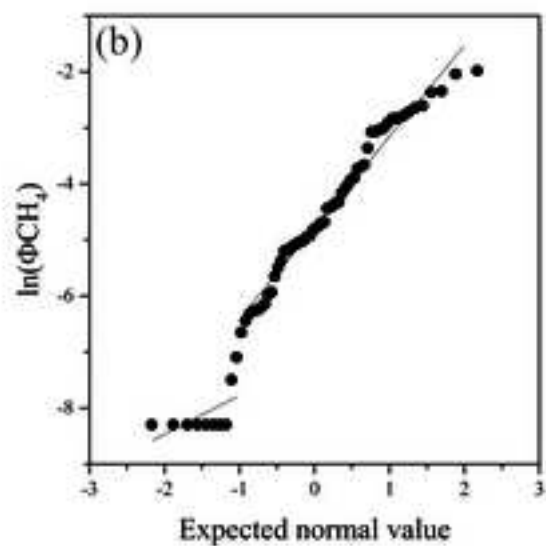
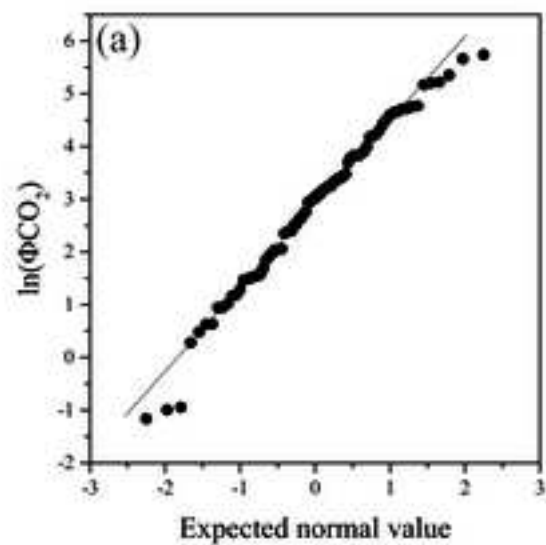


Figure 6  
[Click here to download high resolution image](#)

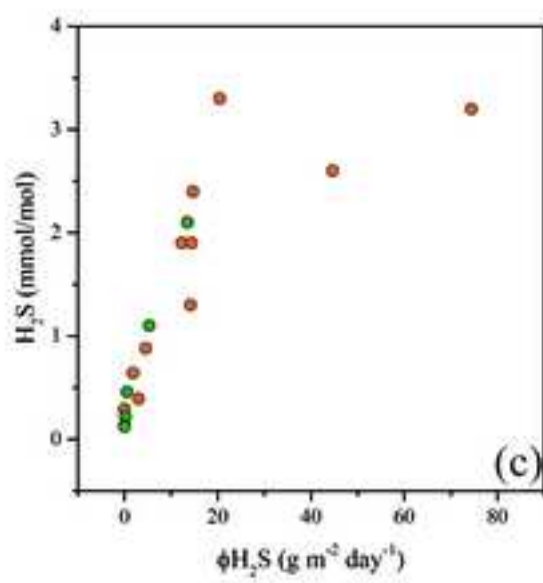
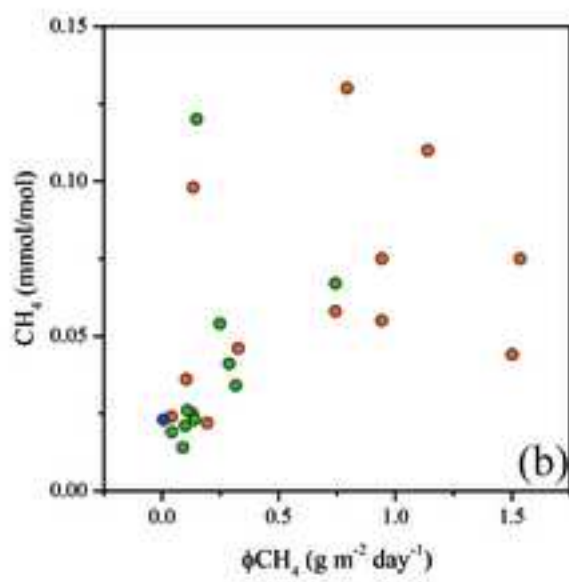
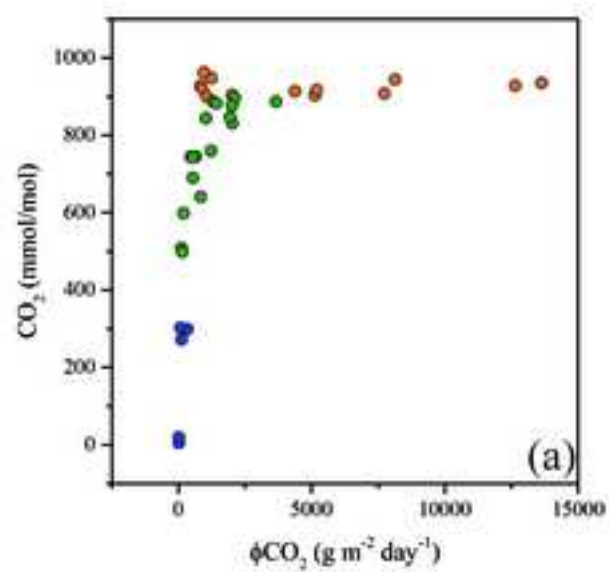


Figure 7  
[Click here to download high resolution image](#)

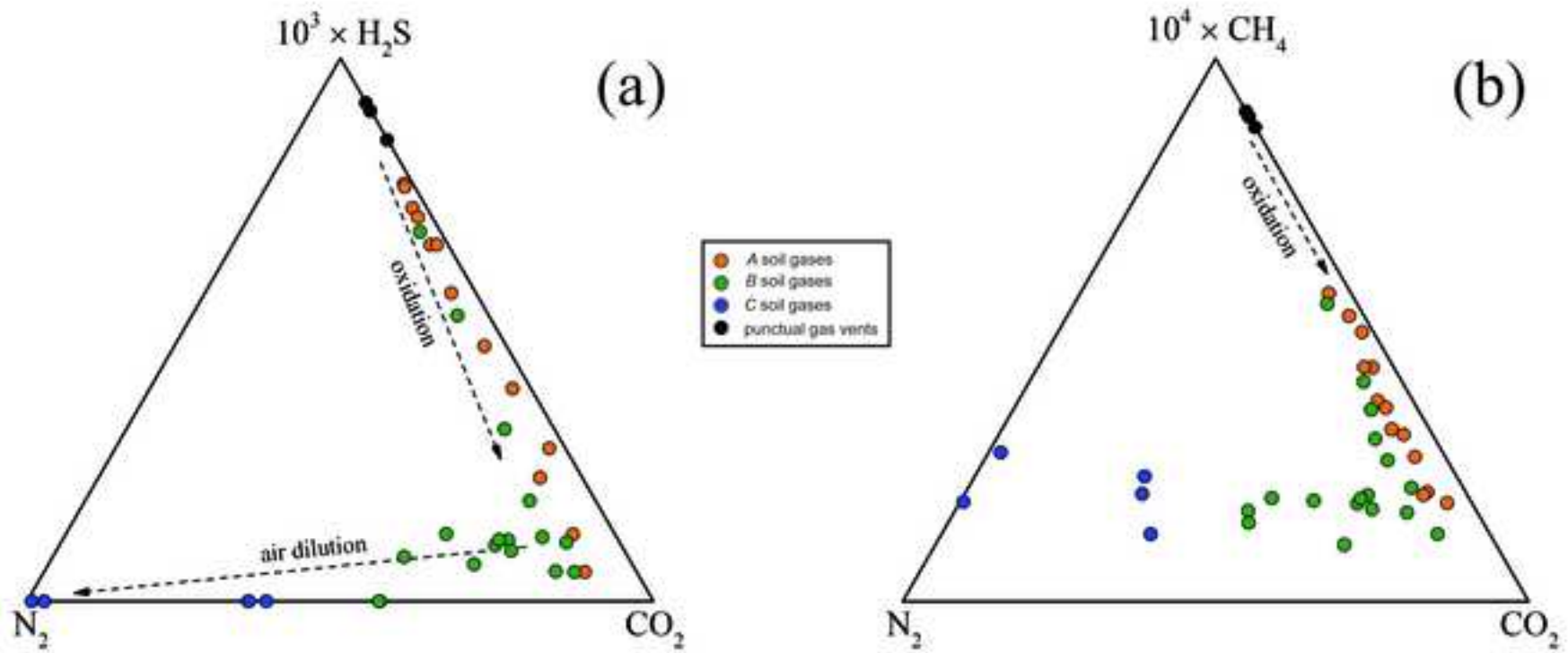


Figure 8

[Click here to download high resolution image](#)

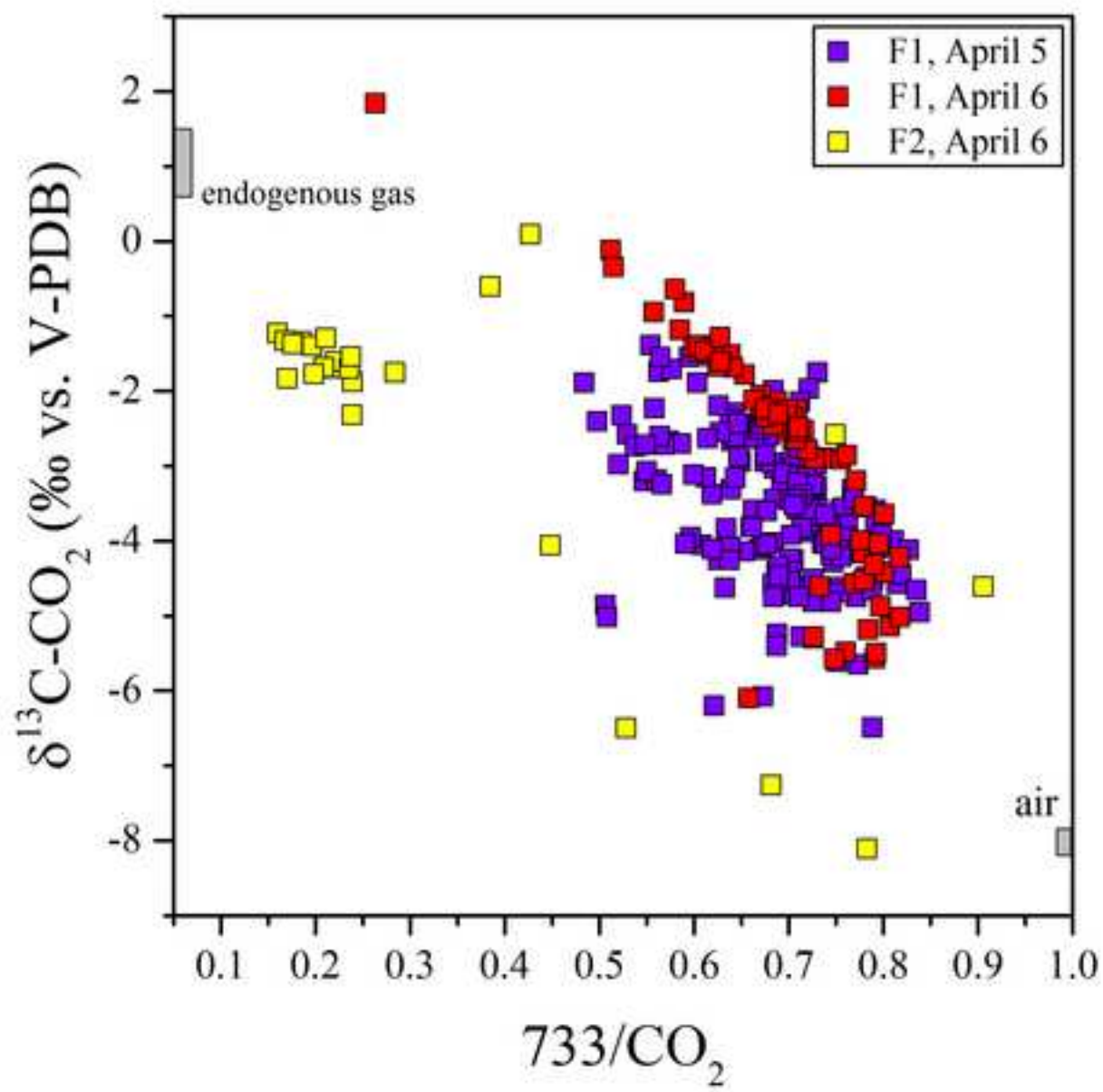




Figure 9  
[Click here to download high resolution image](#)

